TR-O-0120

29

Optical Processing Multibeam Array Antenna

Yu Ji

1996. 3.15

ATR光電波通信研究所

ATR Technical Report

Optical Processing Multibeam Array Antenna
光信号処理によるマルチビームアレーアンテナ

Yu Ji

吉 宇

Radio Communications Department
ATR Optical & Radio Communications Research Laboratories
ATR 光電波通信研究所

Abstract

Recently the application of optical or photonics technology to microwave array antenna in the signal processing and beam formation has been studied. Based on the two-laser model of spatial Fourier optical processing techniques, by placing numbers of optical fibers in the incident focal plane of Fourier transform (focusing) lens, a multibeam optical processing system for microwave transmitting array antennas is proposed in this technical report.

Chapter 1 gives the background of a spatial optical processing antenna and a mathematical description of the antenna characteristics. Chapter 2 presents the structure of optical processor for multibeam array antennas, the general system design and analysis method, and some numerical results, such as optical excitation distribution and antenna radiation patterns. Two-beam experimental optical processor for producing RF signals with different phase distributions and feeding to array antennas is demonstrated in this Chapter as well. By using optical heterodyne process, Chapter 3 describes a parallel optical processor for multibeam antennas, which can greatly reduce the optical alignment difficulties, the free-space beam transmission loss, and the size of the optical processing feed part. To increase the spatial optical sampling efficiency, Chapter 4 proposes a method to produce the bright spots in the image or sampling plane by employing a periodic diffracting mesh. Chapter 5 gives a summary of this technical report.

TABLE OF CONTENTS

1 Spatial Optical Processing Antenna [18]

1.1 Introduction

For future wireless telecommunications, compact, light-weight, flexibly controllable beam forming/steering and large multibeam number antennas are required. Reflector, lens and phased array are three basic generic types of candidates. Comparing with reflector and lens types, array antenna has a number of advantages, such as, higher aperture efficiency, no spillover loss, no aperture blockage and better reliability, but the disadvantages are heaviness, complexity, and higher loss in the power distribution system. To remain the advantages and overcome the disadvantages, the application of optical or photonics technology to microwave array antenna in the signal processing and beam formation has been studied by several institutes for years [1-3]. By using the optical components, the size and heaviness of array antenna can be greatly reduced, and the microwave field distributions on the antenna aperture can be controlled in the optical range.

There are three major techniques for the optically controlled array antenna (OCAA) developments. They are, (I) integrated optical phase and frequency shifters method [4], (II) optical true time delay (TTD) method [5] and (III) spatial Fourier optical processing method [6]. By comparing with techniques (I) and (II), (III) implements the division, interconnection and combination of light spatially, and the individual phase shifter for each radiating element of antenna is not necessary. This will reduce the size and complexity of Beam Forming Network (BFN) system greatly. Therefore, (III) is approved as a more attractive approach for large element and large multiple spot-beam array antennas [7].

The characteristics of beam scanning, beam formation and wideband feature of OCAA have been studied by using approach (III) [8-11]. In this Chapter, the spatial Fourier optical processing technique will be reviewed, and the basic principle of this approach will be presented mathematically.

1.2 Optical Controlled Beam Scanning and Formation

The Fourier transform (FT) lens is used as the main component in the OCAA as shown in Fig. 1-1. The reason of this arrangement is, since the far field radiation pattern of a microwave array antenna is the FT of its aperture distribution, and the amplitude and phase distributions on the aperture are decided by the RF bit signal of two laser beams on the optical fiber array input plane which is the right-side focal plane (image plane) of FT lens, therefore the desired antenna pattern will be achieved by the scaled illuminating mask pattern in the right-side plane of FT lens. The above explanation also can be expressed mathematically in the following.

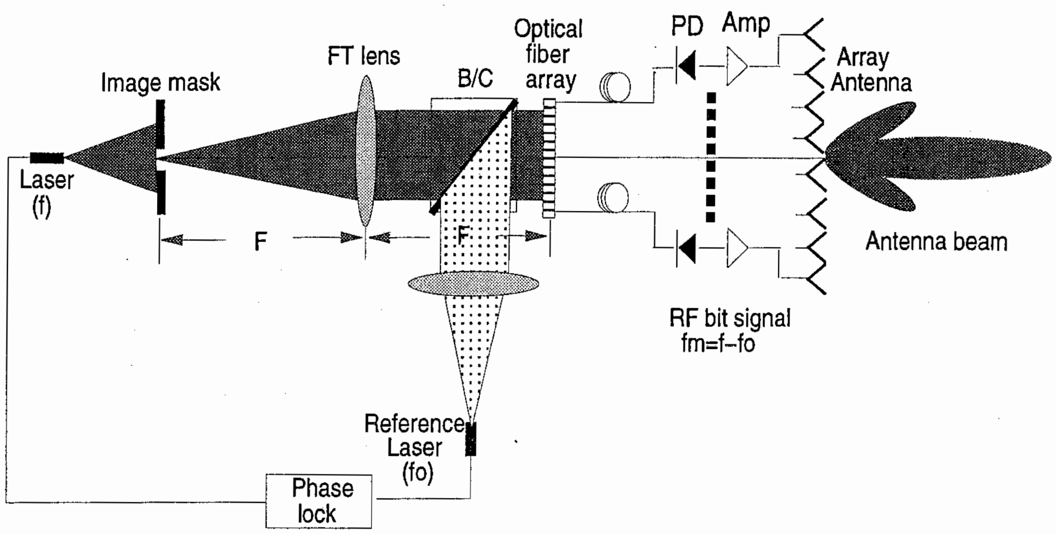

Fig. 1-1 Spatial optical processing array antenna

The field distribution in the right-side focal plane (x_1, y_1) of FT lens is expressed by the FT of the transmittance function t(x, y) in the left-side focal plane (x, y) as

$$E(x_1, y_1) = \iint_D t(x, y) \exp[-j \frac{2\pi}{\lambda_o F}(xx_1 + yy_1)]dxdy, \tag{1-1}$$

where D is the incident field range in the (x, y) plane, and could be the aperture size of mask, λo is the wavelength of the optical light and F is the focal length of the FT lens.

The optical excitation field for microwave antenna is sampled by an optical fiber array on the image plane (x_1, y_1) of FT lens, and then detected by a photodiode (PD) and amplified to feed the radiating elements of array antenna. During this process, optical field is converted to electrical (or microwave) field with the maintenance of amplitude and phase information.

The far radiation field of microwave array antenna is an FT expression of its aperture distribution which is excited by $E(x_1, y_1)$. Then we have

$$F(k_x, k_y) = \iint_{D_a} CE(x_1, y_1) \exp[j(k_x x_2 + k_y y_2)] dx_2 dy_2. \qquad (1\text{-}2)$$

Here we assume that all of the optical field distribution information is sampled by an optical fiber array bundle in the FT lens image plane. In Eq. (2-2), Da is the antenna array size, C is an efficient related to the optical fiber array sampling, PDs and microwave amplifier, and $k_x = \frac{2\pi}{\lambda_m}\sin\theta\cos\phi$, $k_y = \frac{2\pi}{\lambda_m}\sin\theta\sin\phi$ are the components of the wave number in the microwave range.

Since the element number of the optical fiber array which size is D_f equals that of microwave array antenna, the sizes of these two arrays are proportional to each other in wavelength. Therefore, the following relations are obtained as

$$\frac{D_f}{\lambda_o} = m\frac{D_a}{\lambda_m},$$

$$\text{or} \quad \frac{x_1}{\lambda_o} = m\frac{x_2}{\lambda_m}, \quad \frac{y_1}{\lambda_o} = m\frac{y_2}{\lambda_m}, \qquad (1\text{-}3)$$

where m is the beam magnification as defined in [6].

Substituting Eq. (1-3) into Eq. (1-1), Eq. (1-1) can be expressed as the function of x_2 and y_2,

$$E(x_2, y_2) = \iint_D t(x, y) \exp[-j\frac{2\pi m}{\lambda_m F}(xx_2 + yy_2)] dxdy, \qquad (1\text{-}4)$$

On the other hand, by defining (θ, ϕ) as a pair of far-field scanning angles and assuming that θ is small, the following relations in the FT lens part are given according to the discussion in reference [15],

$$\frac{x}{F} = \frac{1}{m}\sin\theta\cos\phi, \quad \frac{y}{F} = \frac{1}{m}\sin\theta\sin\phi. \qquad (1\text{-}5)$$

Then Eq. (1-2) can be rewritten as

$$F(k_x,k_y) = C\iint_{D_a} E(x_2,y_2)\exp[j\frac{2\pi m}{\lambda_m F}(xx_2 + yy_2)]dx_2 dy_2. \tag{1-6}$$

Comparing with Eqs. (1-4) and (1-6), it is easy to find out that these two expressions become forward and inverse FT transform pairs, then we have

$$F(k_x,k_y) = Ct(x,y). \tag{1-7}$$

This equation means that the far field beam patterns can be obtained simply from the same scaled mask patterns. The antenna beam scanning and steering can be realized simply by moving the mask aperture in the focal plane, this is also obvious from the Shift Theorem of FT, and the multi-beam and shaped multi-spot function can be implemented by adding other light sources or making other shaped apertures in the focal plane.

By using the spatial optical processing technique, the amplitude and phase values required for beam forming can be determined simultaneously by means of Fourier Transform capability of focusing lens. But we have point out that the antenna beam scanning is performed by moving the mask pinhole mechanically, and it will effect the scanning speed of antenna.

2 Optical Processor for Multibeam Array Antennas [18], [19]

2.1 Introduction

To increase the capacity of future satellite and land mobile communications base station antennas, the wideband multibeam antennas have been developed for two decades. Because of the advance in printed-circuit antennas and MMIC, active phased arrays tend to be alternatives to reflectors and lenses. However, this makes the Beam Forming Network very complicated, heavy and expensive.

Recently, the application of optical or photonics technology to produce multibeam microwave array antennas has been studied [12]～[14]. Instead of full use of microwave components, optical components such as lenses and fibers are employed to control the phase and amplitude weights for each element of the array. In this Chapter, firstly an optically controlled multi-beam BFN system which is based on the two-laser model Fourier optical processing technology [15], [16] is proposed by introducing other optical laser fibers in the input focal plane of Fourier Transform (focusing) lens. The general system design and analysis method will be given by using Fourier optics. By connecting this system to a large-element-number array antenna, according to the laser sources, simultaneous, independent and frequency diverse multiple beams will be produced in the desired directions. Secondly the condition of generation of contiguous multibeam in this system and numerical calculation results of optical excitation distribution and antenna radiation patterns versus some particular system parameters, such as the arrangement of input laser fibers and sampling optical fiber array, are given. Finally an experimental system for two-multibeam array antenna are described and the RF signals which will feed the microwave array antenna are detected by photodetector, and the measured results of optical excitation amplitude and phase distributions with a comparison of simulation results will be given.

2.2 System Design and Analysis

Since the various arrangement of input laser beams in the left-side focal plane of FT lens can control the antenna radiation characteristics as shown in Chapter 1, if we place n optical fibers as signal sources with different frequencies f_1, f_2, ..., f_n in the left-side focal plane of FT lens, and lock the laser sources to the reference laser with individual frequency offset, the multiple beams from array antenna will be produced with individual microwave (RF) frequencies f_{m1}, f_{m2}, ..., f_{mn} as shown in Fig. 2-1.

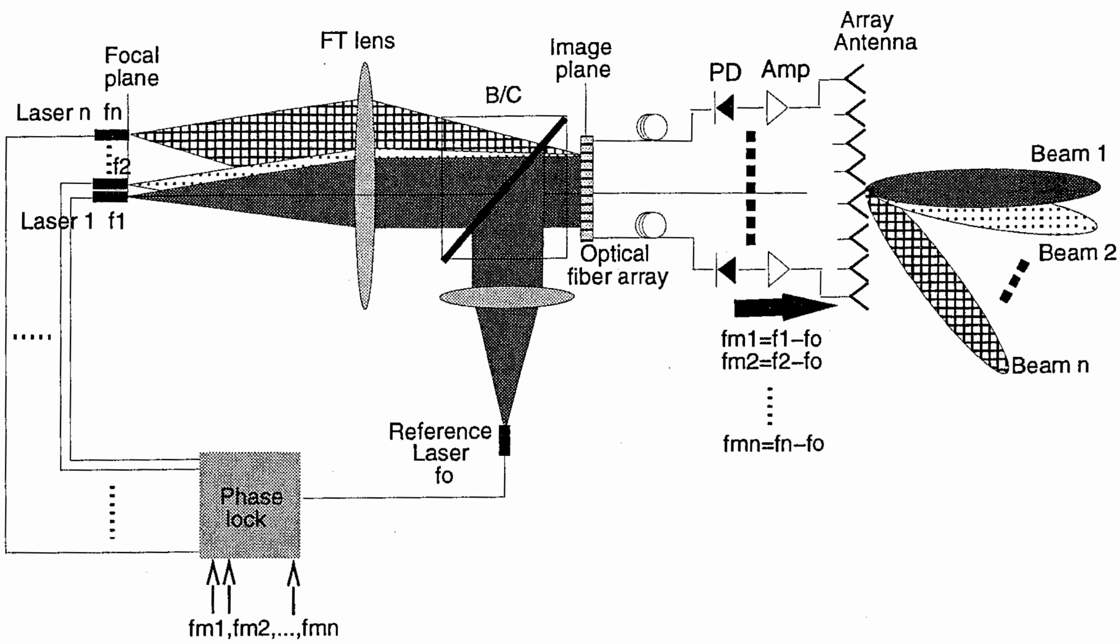

Fig. 2-1 Multibeam BFN system for array antenna

The functional block diagram of the optical feed for a multibeam microwave array antenna is shown in Fig. 2-1. The *n* optical fibers connecting to different master lasers are placed in the left-side focal plane (x_0, y_0, z_0) of the FT lens, and their center is r_0 from the optical axis. The emitting optical beams from the fibers will be Gaussian distribution beams. After transmitting to the FT lens, the beams will focus in the image plane with the same Gaussian intensity and different phase distributions, as shown in Fig. 2-1. Each master laser phase-locks to the reference laser with an individual frequency offset and corresponds to the difference working frequency antenna multibeam. The optical beams from the master lasers and the reference laser are mixed at Beam Combiner (B/C) and are incident on a sampling fiber array placed in the image focal plane (x_1, y_1, z_1) of the FT lens. The frequency differences between optical beams from the master lasers and the reference laser as RF beatnote signals will be detected by a photodetector and feed to the radiating elements of a microwave array.

To increase the antenna gain and reduce the antenna covering open space, the generation of multiple overlapping beams is necessary [17]. Because of the structure of standard single-mode optical fiber in which the diameter of core is only 10 μm comparing with 125 μm of cladding, just simply placing the optical fibers in the focal plane of FT lens can not produce overlapping antenna beams. To solve this difficulty, a GRIN (GRadient INdex) lens is employed to connect with the incident emitting fibers, so that the small beam-spots will expand to large contiguous beams in the focal plane and a plane wave front is maintained as shown in Fig. 2-2. This design can also increase the emitting power on the FT lens.

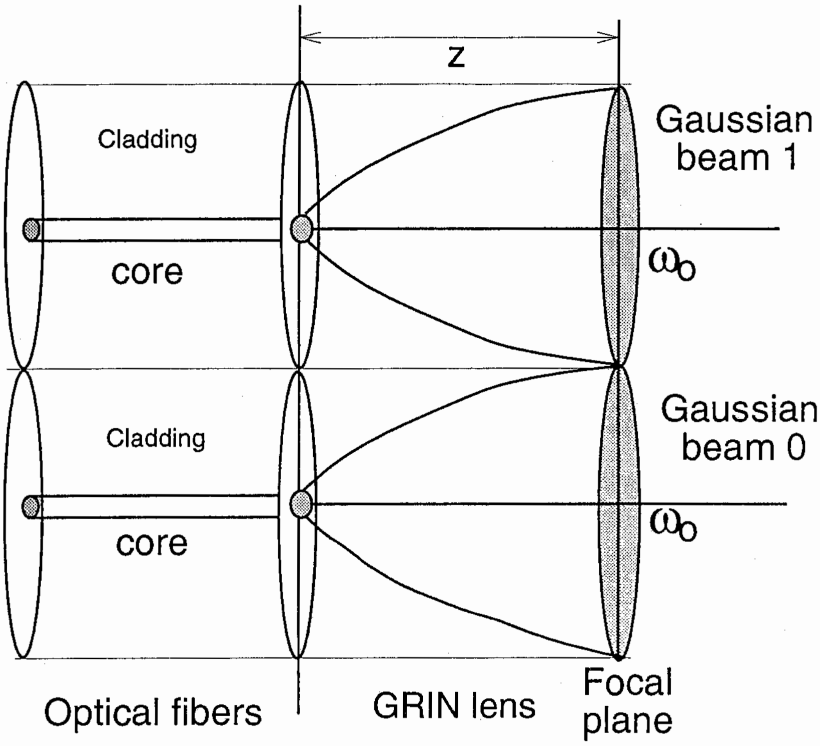

Fig. 2-2 Expansion of Gaussian beam in the focal plane of FT lens

To simulate the multibeam patterns of array antenna, the optical excitation distribution in the image plane is a key point. From Eq. (1-4), the optical field distribution in the image plane of FT lens caused by a truncated Gaussian beam from an optical source which is r_0 offset from the optical axis can be expressed as

$$E(r_1) = \exp(j2\pi r_1 r_o / \lambda_o F)\int_0^{\omega_o} e^{-r^2/\omega_o^2} J_0[2\pi r r_1 / \lambda_o F] r dr, \qquad (2\text{-}1)$$

where ω_0 is the expanded beam waist in the left-side focal plane and J_0 is the zero-order Bessel function.

If the image mask in the left-side focal plane has a circular pinhole aperture, the incident beam to FT lens will have a uniform amplitude distribution, and Eq. (2-1) will be further reduced as first-order Bessel function as described in [16].

When we assume that the beam emitted by an optical fiber is a perfect Gaussian beam, the amplitude of the optical beam is a Gaussian distribution with beam waist ω_0, and the optical field excitation in the image plane of the FT lens caused by an arbitrary incident optical fiber can be expressed as

$$E(r_1) = \exp(j2\pi\vec{r}_1 \bullet \vec{r}_0 / \lambda_0 F) e^{-r_1^2/\omega_1^2} \tag{2-2}$$

where λ_0 is the optical wavelength, F is the focal length of the FT lens, and the beam waist radius in the image plane is given as

$$\omega_1 = \lambda_0 F / \pi\omega_0 \tag{2-3}$$

The optical field distribution E in Eqs. (2-1) and (2-2) in the image plane of FT lens contains both amplitude and phase part. When E is sampled by an optical fiber array with N elements, the excitation field for n-th array element can be written as

$$E_n(x_1, y_1) = A_n e^{j\alpha_n} \tag{2-4}$$

Through the PD and amplifier, E_n becomes the aperture field illumination of n-th antenna array element. Therefore, the far-field radiation field from a linear array antenna is given as

$$R(\theta) \propto \sum_{n=0}^{N} A_n f_n(\theta) \exp[j(nkd_m \cos\theta - \alpha_n)] \tag{2-5}$$

where $f_n(\theta)$ is the n-th element radiation pattern function, k is the wave number in the microwave range and d_m is the distance between two antenna elements.

2.3 Numerical Results and Discussion

The numerical analysis of multibeam antenna and design of system parameters will be carried out in this section. The standard system parameters are given as: ω_o=62.5 μm, F=120 mm, λ_o=1.3 μm, the interval x_o between emitting fiber centers and the distance d_o between fiber cores of sampling fiber array elements are 125 μm, and $d_m=\lambda_m/2$. The number of array elements will be discussed from 9 to 161 in one dimension. The radiation pattern function in Eq. (2-5) for each radiation element is assumed as a sine function.

When three truncated Gaussian beams with beam waist ω_0=62.5 μm are incident, the beam centers are 0 μm, 125 μm and 250 μm away from axis, respectively. The calculated amplitude and phase distributions of the optical excitation field in the image plane of FT lens are shown in Fig. 2-3. For these three beams, because all of beams are focused in the focal (image) plane, the same optical field amplitude distribution for different incident beams is obtained in this particular plane, in the range -10 mm～10 mm. Comparing truncated Gaussian beams incidence and uniform distribution beams incidence, there is no big difference in the main amplitude patterns around the axis, but the sidelobe levels related to truncated Gaussian beams are quite lower. The phase distributions are calculated in the main amplitude pattern range (-1 mm～1 mm). We find that they change linearly with the location of incident beams, but keep the same distributions when the different style beams are incident.

Fig. 2-4 shows the multibeam antenna patterns which are normalized by the power pattern when the incident beam is on the optical axis, when element number, incident Gaussian beam radius and interval between fiber array elements are changed. Figs. 2-4 (a) and (b) show that, when the array elements are increased, the side-lobe of antenna pattern will reduce and main beam width will become narrower, but there is no change on the multiple beam directions if the incident fiber locations are fixed. From Fig. 2-4 (c), we find that, when the interval between fiber array elements is reduced, the interval between antenna beams becomes smaller as well.

Fig. 2-5 presents the Half-Power Beam Width (HPBW) of the antenna radiation patterns versus the number of array elements and the incident beam radius. This figure shows that the antenna beam width not only depends on the antenna size but also the controlling optical beams.

The fiber locations and corresponding antenna beam directions are shown in Table 2-1, where the last column data are calculated from Eq. (1-5).

From Table 2-1, we find that if the sampling phase difference is less than 180^0, the optical field information will be transferred to the sampling fiber array correctly and a controllable beam will be generated, therefore, a big Field of View (FOV) (-75°～75°) which is covered by multiple beams can be obtained by this type of OCAA. In this case, the maximum number of multiple beams is 11×11=121. If the emitting fibers are instituted for smaller interval open-ended optical wave-guides, larger number multiple beams could be realized.

Table 2-1. Arrangement of laser fiber sources and corresponding antenna beam directions

Fiber No.	Distance from optical axis (μm)	Sampling phase difference	Beam direction	Evaluated Beam direction
0	0	0°	0°	0°
1	125	36°	11.60°	11.56°
2	250	72°	23.66°	23.61°
3	375	108°	37.00°	36.94°
4	500	144°	53.30°	53.25°
5	625	180°	75.00°	80.25°

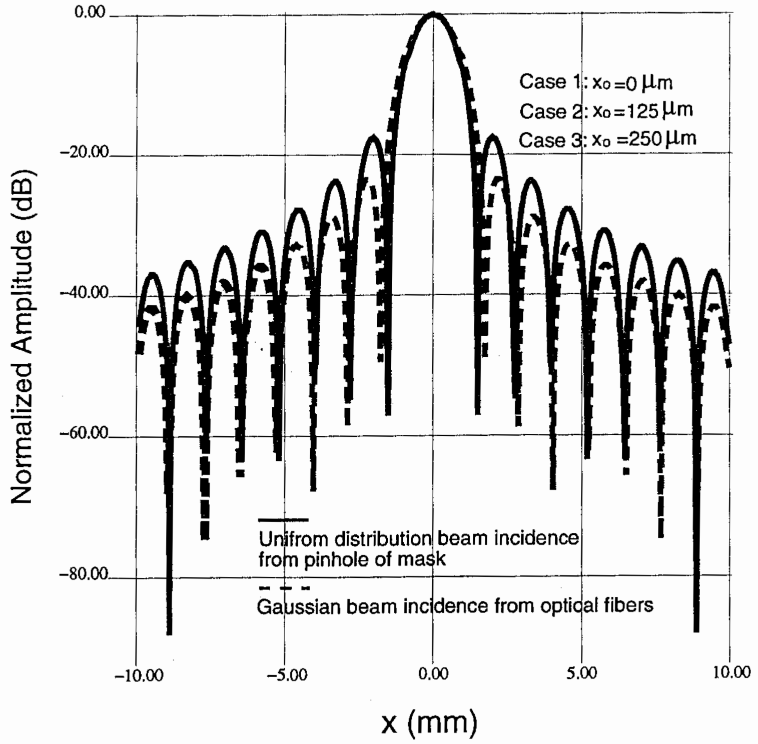

(a) Amplitude

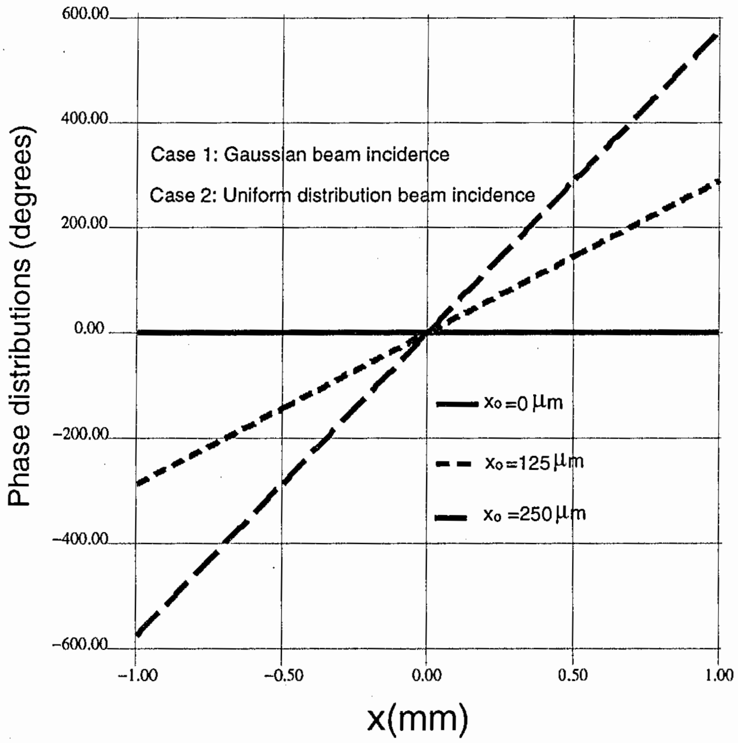

(b) Phase

Fig. 2-3 **Optical excitation field distributions in the image plane of FT lens**

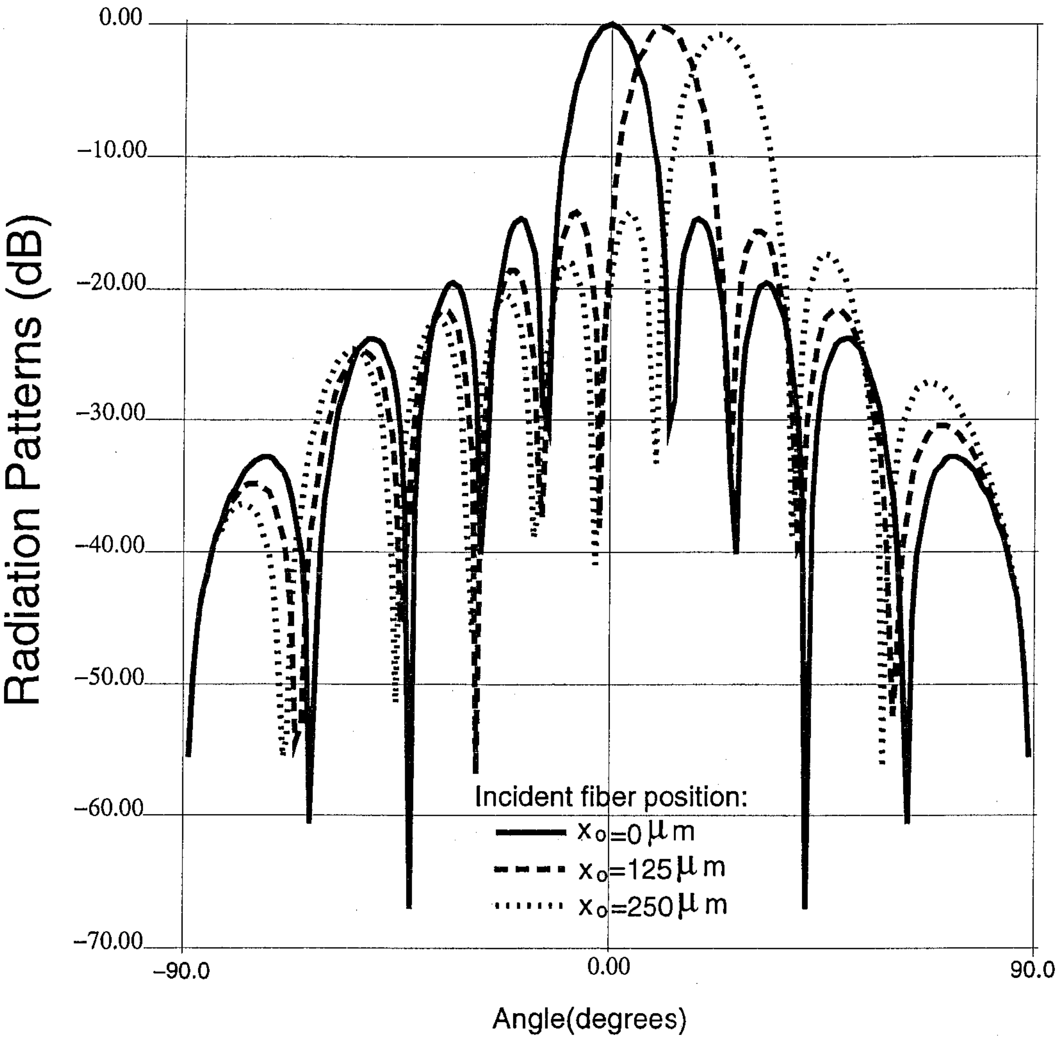

Fig. 2-4 (a) Multibeam array antenna patterns when F=120mm, N=9, ω_0=62.5μm, d_0=125 μm

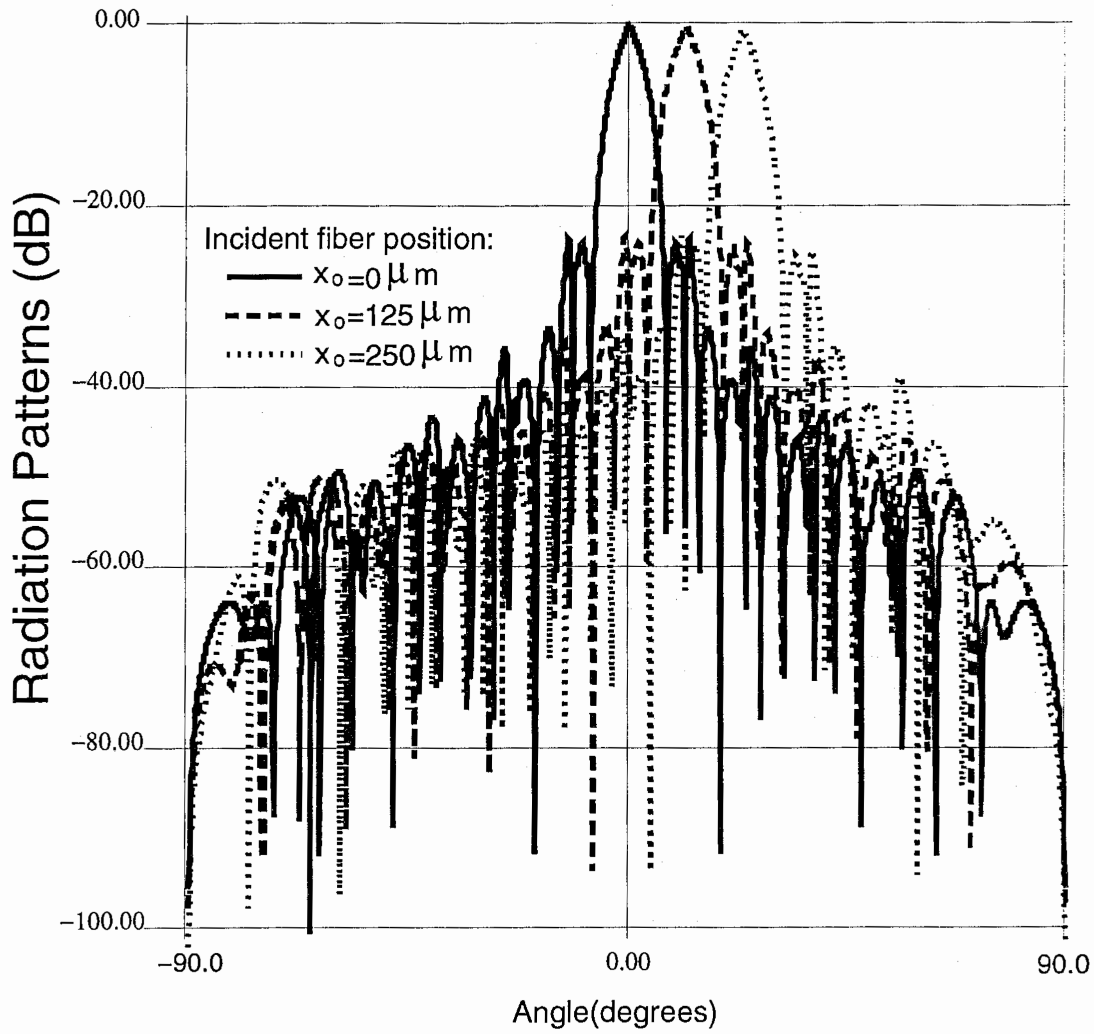

Fig. 2-4 (b) **Multibeam array antenna patterns when F=120mm, N=161, ω_o=62.5μm, d_o=125μm**

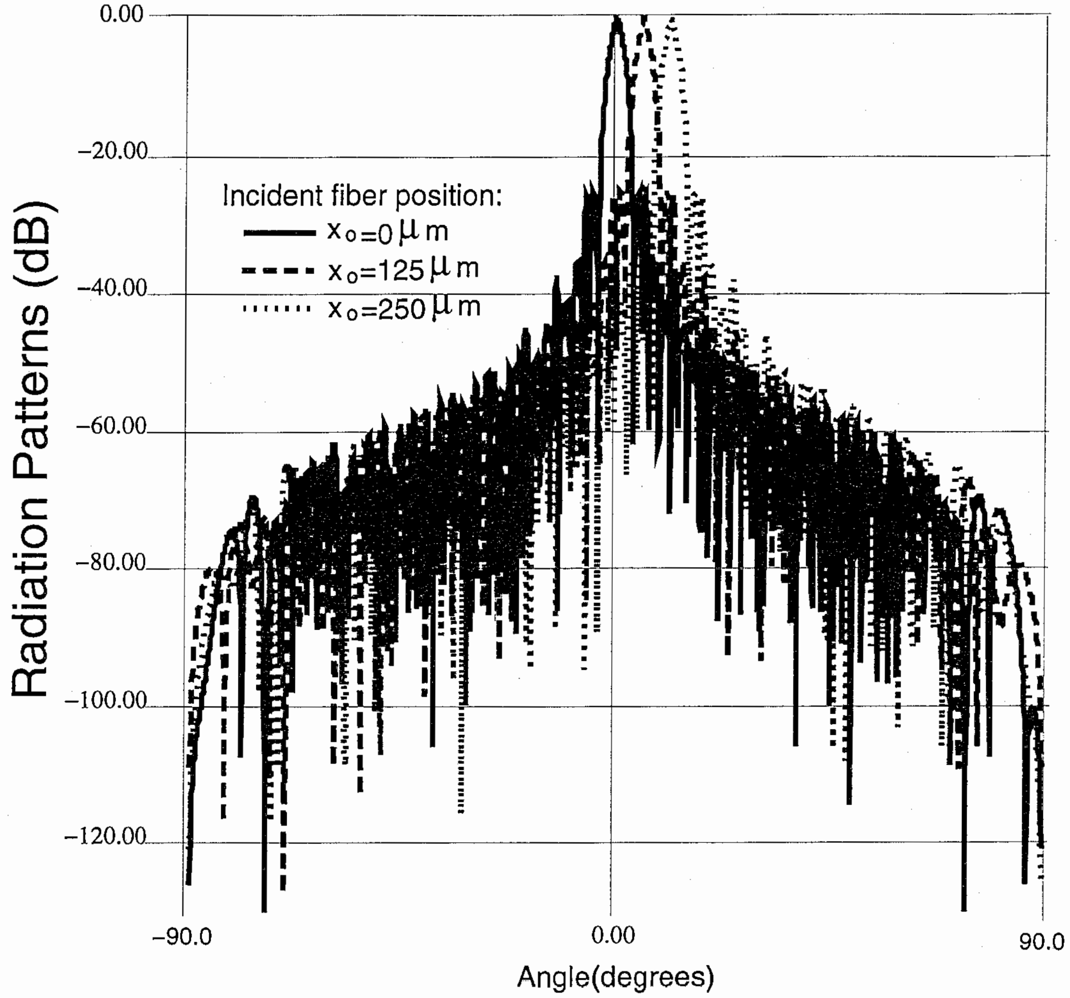

Fig. 2-4 (c) **Multibeam array antenna patterns when F=120mm, N=161, ω_0=62.5μm, d_0=62.5μm**

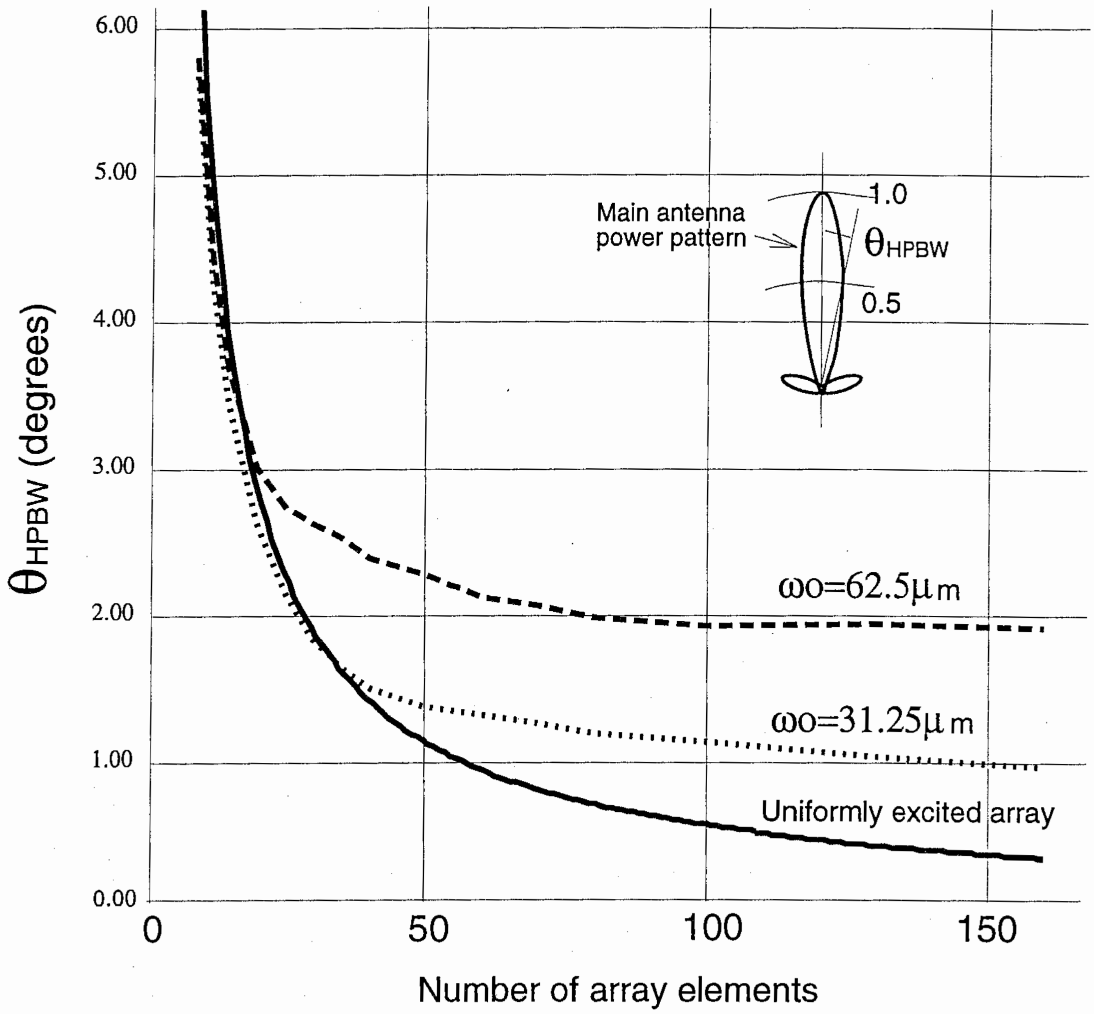

Fig. 2-5 **Half-Power Beam Width (HPBW) of antenna radiation patterns versus the number of array elements and the incident optical beam radius**

2.4 Experimental system and Results [19]

The optical feed experimental arrangement for a microwave array antenna is shown in Fig. 2-6. As the optical sources, three LD pumped Nd:YAG lasers in the 1.319 μm region with output power of roughly 50 mw are used. One works as the reference beam, the other two as master lasers phase locked to the reference laser and the frequency differences are set to 800 MHz and 1 GHz separately. Single mode optical fibers with a GRIN lens with a diameter of 125 μm are used to emit the optical beams. The focal length of both lenses is 120 mm. The width of the Gaussian beams in the image plane can be calculated as 794.5 μm from Eq. (2-3).

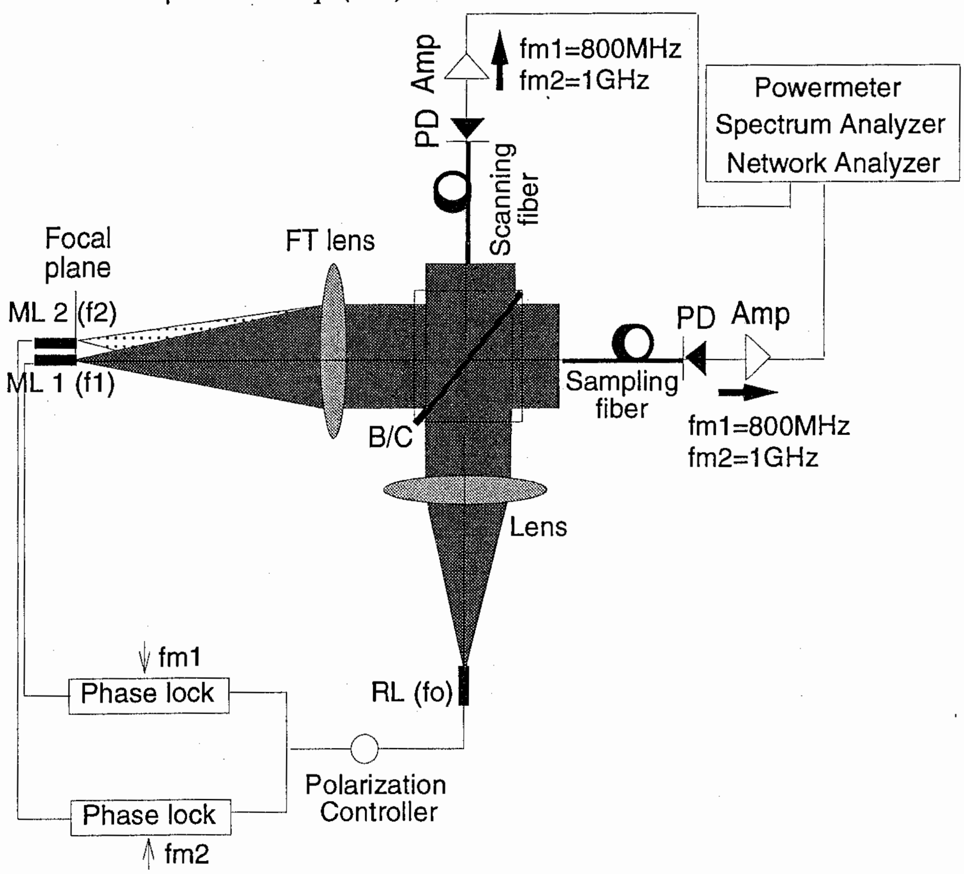

Fig. 2-6 Experimental arrangement

A complete optical heterodyne system consists of two main components: two lasers whose output is mixed together to produce a difference frequency (beatnote signal), and a method of precisely controlling those two lasers to give the desired frequency. A Lightwave's Laser Offset Locking Accessory can control the difference in optical frequencies between two tunable lasers and phase-locks this difference to a specified RF frequency.

To generate a beatnote signal between free-space lasers, their beams must be almost the same size, have the same polarization direction, and most importantly be collinear. In our experimental system, all of these conditions are satisfied. The RF signals are detected by the sampling fiber after laborious optical alignment and the results are shown in Fig. 2-7.

Both the measured and calculated amplitude and relative phase distributions of these two RF signal excitations are shown in Fig. 2-8 and Fig. 2-9. This information will be sampled by an optical fiber array and feed to the microwave array antenna. The radiation patterns and directions of the multibeam are determined by the excitation amplitude and phase distributions, respectively. Certainly by introducing an extra signal source, the RF signals from several GHz up to millimeter wave range could be generated.

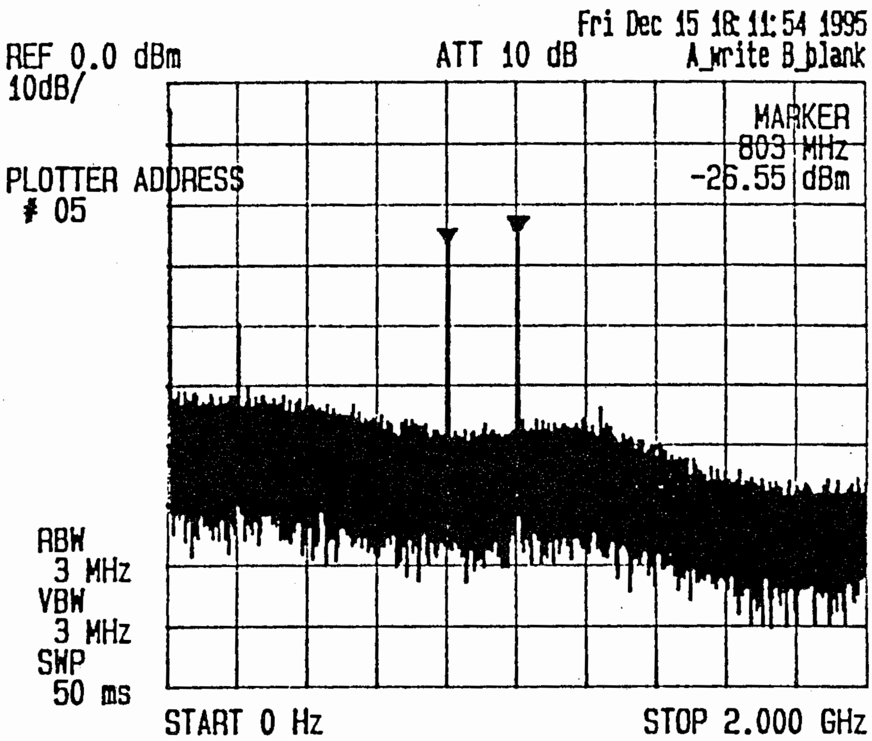

Fig. 2-7 Multibeam RF signals detected at 800 MHz and 1 GHz.

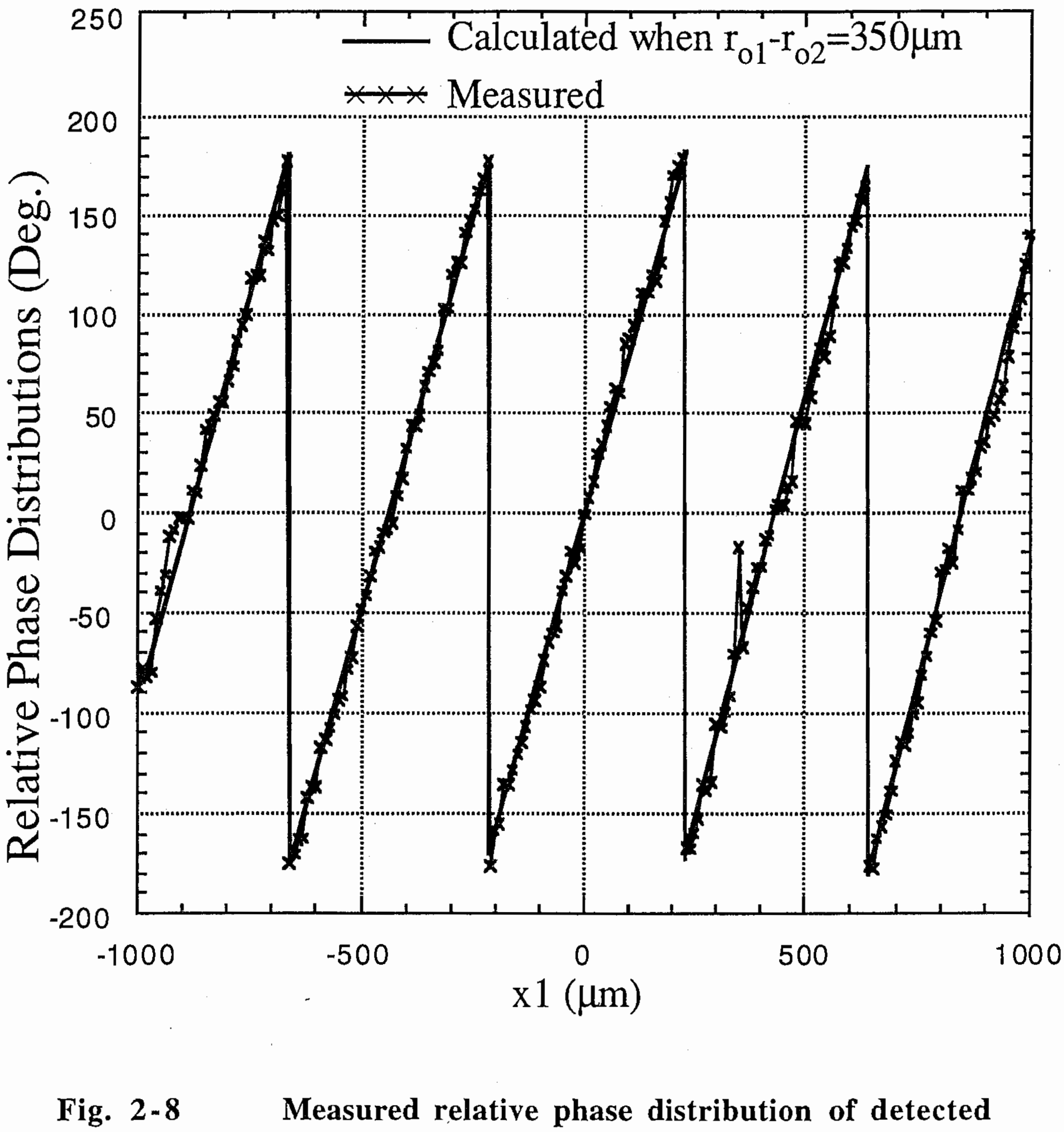

Fig. 2-8 **Measured relative phase distribution of detected RF excitation signals**

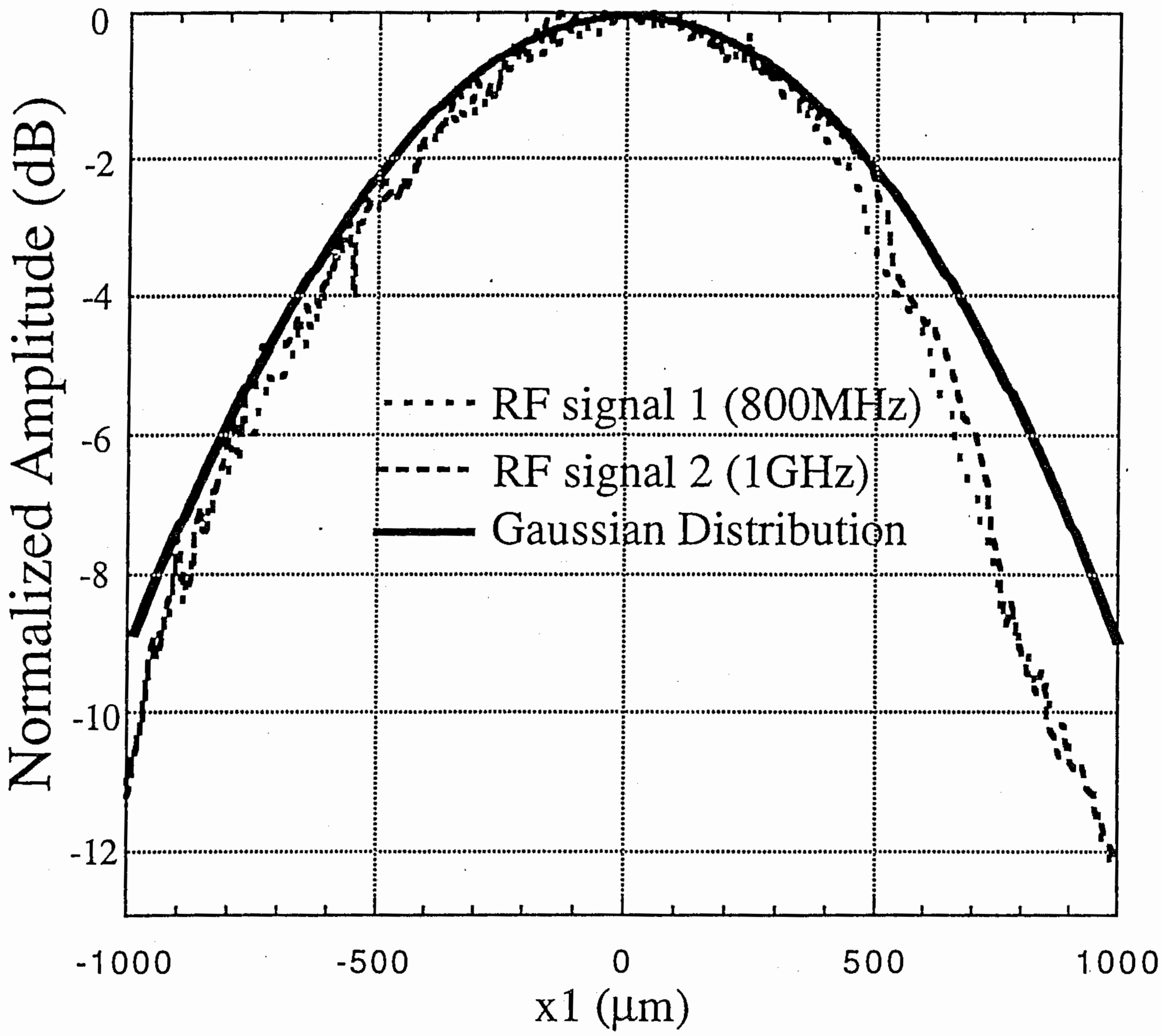

Fig. 2-9 Measured field intensity of detected RF excitation signals

3. Parallel Optical Processor for Multibeam Array Antennas [23]

3.1 Introduction

In recent years significant progress has been made worldwide on the application of the optical or photonic technology to microwave phased array antennas. A number of approaches have been proposed in beam-forming, beam-scanning, RF signal distribution and the remote control of the antenna. The advantages of using optics in array antennas are extremely wide bandwidth, miniaturization in size and weight and immunity from electromagnetic interference and crosstalk.

By applying spatial optical processing technique, the optical-fed multibeam array antennas which could be used as a satellite-on-board antenna or mobile communication base-station are developed recently. In the conventional microwave Beam Forming Network (BFN), the more the beams are produced, the more complicated matrix circuit, the more interconnection numbers and the larger BFN are required. For large number multibeam array antenna, how to reduce the BFN size and weight is a vital problem. In the optical BFN, an optical lens replaces the matrix circuit to implement the beam division, interconnection and combination spatially. When the beam number increases, only the lasers equivalent to the number of microwave beams are required, and there is no change in the BFN part. Both the simulation and experimental results have demonstrated the effectiveness of this structure [18-20]. However, there are two problems when we set up the real antenna system. One is the laborious alignment for producing the same size and collinear optical beams spatially. Another is the power loss of the beam transmission in the free space. To solve these two difficulties, in this paper we propose a new design using optical heterodyne processing technique. In this design, the emitting optical fibers from both the master lasers and the reference laser will be arranged in the same axis in parallel.

The optical heterodyne processing principle, system parameter design and the experimental results will be presented in this Chapter.

3.2 Optical Heterodyne Process

To generate and control a microwave signal with a particular phase shift, the optical heterodyne is a very effect procedure [21]. This process needs two frequency offset optical beams which could be from the same laser source or from two phase locked laser sources [22]. When these two laser beams from different directions are incident on an optical fiber array, a moving sinusoidal interference pattern will be generated and sampled by each of fiber, and the moving rate equals to the offset frequency. The RF signal with a phase shift determined by the incident angles can be detected by photodetectors connecting to fiber array.

We propose a new type of optical heterodyne processor for multibeam array antennas. Fig. 3-1 illustrates the system diagram in which only one focusing lens is employed to focus the beams from both master lasers and reference laser and the beam combiner used in the conventional design is omitted. As a possibility, the fiber connecting to the reference laser is placed on the optical axis, and the fibers connecting to master lasers are around it. This design will greatly reduce the optical alignment difficulties, the free-space transmission loss, and the size of the optical processing feed part. Next we will go details of the processor design and find the optimal system parameters for the purpose of producing multiple beams.

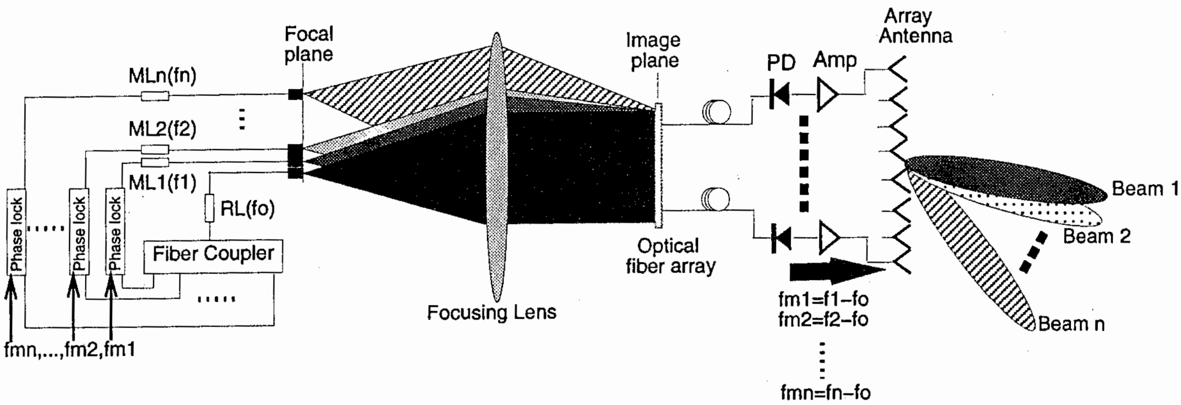

Fig. 3-1 Proposed optical signal processor for multibeam array antenna

In the optical heterodyne processing, to produce stable RF signals effectively, two incident optical beams with different incident angles should have the same polarization. Then the incident beams as plane polarized waves on the sampling plane can be written as

$$\vec{E}_r = \vec{i}_x A_r e^{j\Omega_o t} \tag{3-1a}$$

and $$\vec{E}_m = \vec{i}_x A_m e^{j\Omega_1 t + jk\sin\theta_1} \tag{3-1b}$$

respectively, where Am and Ar are amplitudes of the master and reference beams respectively, θ is the beam interference angle.

In the image plane of the focusing lens, the master and reference beams with the same beam radius are mixed together, and the total field is the superimposing of Eqs. (3-1a) and (3-1b) as

$$\vec{E}_T = \vec{E}_m + \vec{E}_r = \vec{i}_x (A_m e^{j\Omega_o t} + A_r e^{j\Omega_1 t + jk\sin\theta r_1}), \tag{3-2}$$

and the total field intensity is given by

$$\begin{aligned} I = \vec{E}_T \bullet \vec{E}_T^* &= (A_m e^{j\Omega_o t} + A_r e^{j\Omega_1 t + jk\sin\theta r_1})(A_m e^{-j\Omega_o t} + A_r e^{-j\Omega_1 t - jk\sin\theta r_1}) \\ &= 2A_m A_r + 2A_m A_r \cos(\Omega_m t + 2\pi r_o r_1 / \lambda F) \end{aligned}, \tag{3-3}$$

where the frequency difference $\Omega_m = \Omega_1 - \Omega_o$ is set as the desired antenna RF frequency. When this mixed optical signals are input to a photodetector, the output photocurrent is proportional to the intensity $A_m A_r$, and the beat signal of Ω_m is detected to produce a source of GHz frequencies.

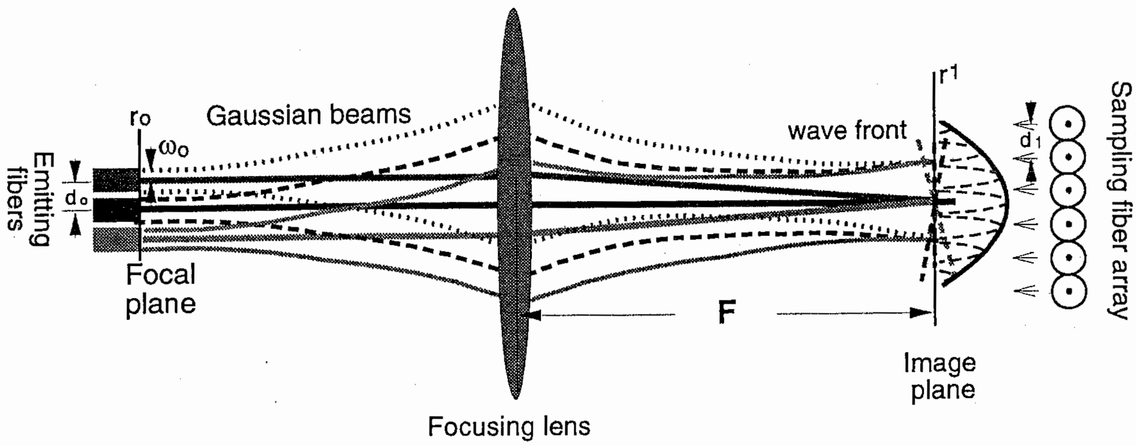

Fig. 3-2 Parallel optical processing of Gaussian beams by using focusing lens

Since the amplitudes of the optical beams from a single-mode fiber in section have Gaussian distributions, and an ideal lens only changes the beam size but not the beam mode, so after the transmission through the lens, the beams will keep the Gaussian mode unchanged. Therefore, the field amplitude in Eq. (3-1) as the optical excitation of the array antenna can be written as $A_m(or\ A_r) = A_{mo}(or\ A_{ro})e^{-r_1^2/\omega_o^2}$ and $\omega_1 = \dfrac{\lambda F}{\pi\omega_0}$, where ω_o is the beam waist and F is the focal length of the lens. If the distance r_o from incident fibers to the optical axis is much smaller than the focal length F of focusing lens, we have $\sin\theta = \theta = r_o/F$. Fig. 3-2 shows how three Gaussian beams, the one on the axis is the reference beam and the others are master beams, transmit to a focusing lens and mix together in the image plane. The dotted lines inside of solid Gaussian distribution are the moving sinusoidal interference patterns.

3.3 System Parameters Evaluation

Although there is no design condition of sampling fibers to be required for sampling the optical field distributions, but to pick up the RF signals which equals to the moving interference pattern rate, at least one sampling fiber should be placed between each of the nulls of interference pattern. Therefore, we have a condition for system parameters

$$\frac{d_1 r_o}{F} \le \frac{\lambda}{2}\ , \qquad (3\text{-}4)$$

where d_1 is the distance between two adjacent sampling fiber centers. Therefore, the maximum number of multiple beams in one dimension which can be produced by the microwave array antenna will be decided by

$$M = \frac{\lambda F}{d_o d_1}\ , \qquad (3\text{-}5)$$

where d_o is the distance between two adjacent emitting fiber centers.

From the well known Shift Theorem of a focusing lens, that is, a spatial change of the field in the focal plane of one side introduces a linear phase shift in the focal plane of another side, the optical interference excitation field distributions in the sampling plane (x_1, y_1, z_1) by mixing an arbitrary master beam and a reference beam can be expressed as

$$E_o(r_1) = A_{mo}A_{ro}e^{-2r_1^2/\omega_1^2}e^{j2\pi\vec{r}_1\cdot\vec{r}_o/\lambda F}. \qquad (3\text{-}6)$$

where r_o denotes the location of the fibers emitting the master laser beams.

The real part in Eq. (3-6) refers to the instantaneous interference patterns which move with time by the rate of frequency difference between the two lasers.

Since about 95% power concentrates in the beam waist of Gaussian beam, the element number of both sampling fiber array and microwave antenna array can be decided by

$$N = \frac{2\omega_1}{d_o} = \frac{2\lambda F}{\pi d_o \omega_o} \tag{3-7}$$

Since the instantaneous light interference pattern sampled by the fibers will be time-averaged as a Gaussian distribution by photodetectors, the far-field radiation pattern of the microwave array antenna is given by

$$E_R(\theta) = \sum_{n=-N}^{N} A_{mo} A_{ro} e^{-2n^2 d_1^2 / \omega_1^2} \exp[jnk(d_m \cos\theta - \frac{d_1 \hat{r}_1 \bullet \bar{r}_o}{F}), \tag{3-8}$$

where the total element number of both the optical sampling fiber array and the microwave antenna array is decided by $2N+1 = \frac{2\lambda F}{\pi d_o \omega_o}$, and d_m is the interelement spacing of the antenna array.

3.4 Numerical and Experimental Results

The instantaneous light interference patterns between the master beams emitted from the fibers with a GRIN lens 125 μm from the optical axis, and the reference beams from the fiber on optical axis are shown in Fig. 3-3. The GRIN lens is employed to produce overlapping multiple beams and reduce the power loss as discussed in Chapter 2.

Numerical simulated multibeam radiation patterns of three overlapping multiple beams are shown in Fig. 3-4. Through numerical calculations, some trends on antenna radiation patterns have been found: (a) as F increases, the main lobe narrows and the side lobe level increases; (b) as N increases, the main lobe narrows and the side lobe level decreases: (c) as d_1 increases, the main lobe widens and the side lobe level decreases.

Variations of the maximum number of multiple beams and the number of sampling fibers or antenna elements versus the distance between sampling fibers and the focal length of the focusing lens are shown in Figs. 3-5 and 3-6, respectively. These graphs indicate that the number of multibeams and the antenna size can be increased greatly by integrating a sampling fiber array to an optical waveguide array.

A two-beam optical processor has been set up. Three single-mode fibers, which are connected to three LD pumped Nd:YAG tunable lasers in the 1.319 μm region with output power of roughly 50 mw, were fixed as close as possible in parallel in one focal plane of a lens. Two master lasers were phase-locked to a reference laser with frequency offsets of 900 MHz and 1 GHz separately. The three laser beams transmit through a focusing lens, mix together spatially, and then are sampled by a lens-ended optical fiber. The spectra of multiple relatively high level RF signals are shown in Fig. 3-7 as detected by a photodetector.

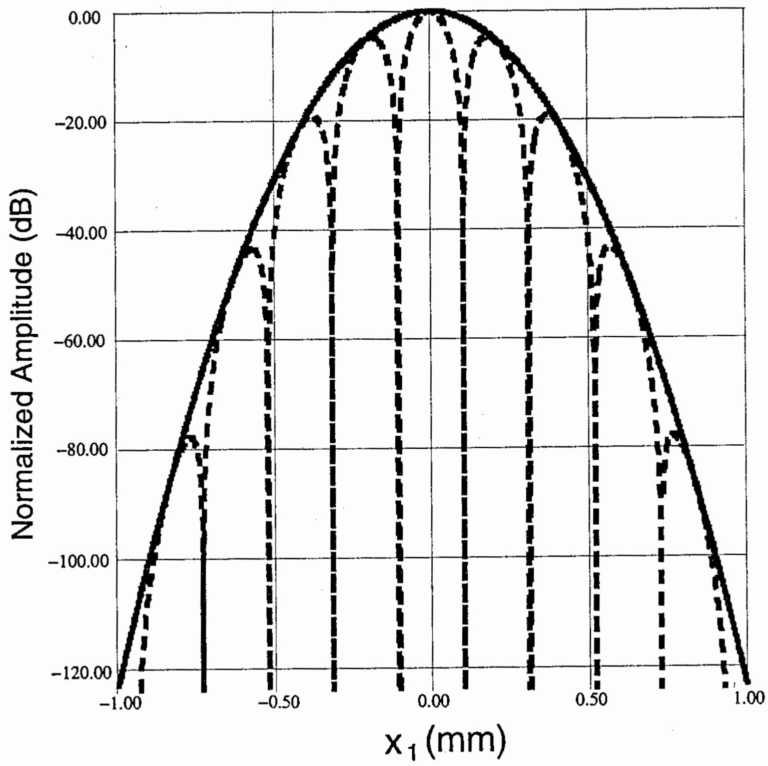

Fig. 3-3 **Light interference pattern (dotted) with Gaussian envelope (solid) in the image plane of focusing lens.**

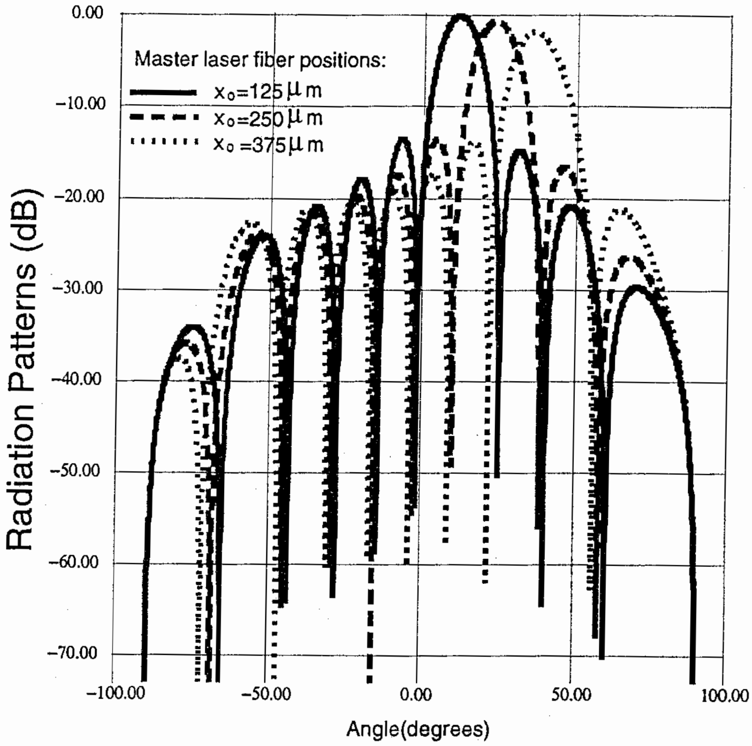

Fig. 3-4 Calculated microwave array antenna multibeam patterns, where the element number of antenna array N is 9.

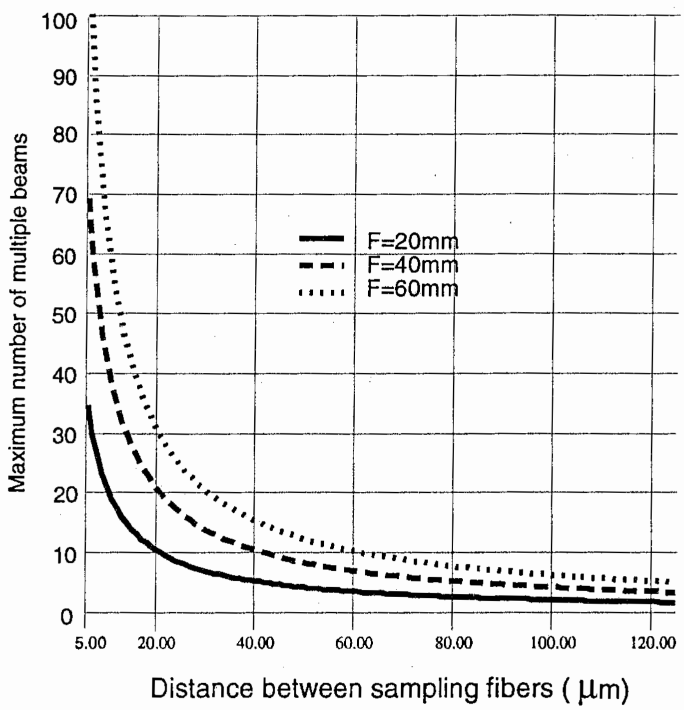

Fig. 3-5 Variations of maximum number of multiple beams versus the spacing between sampling fibers and the focal length of focusing lens, when λ=1.3 μm, do=125 μm.

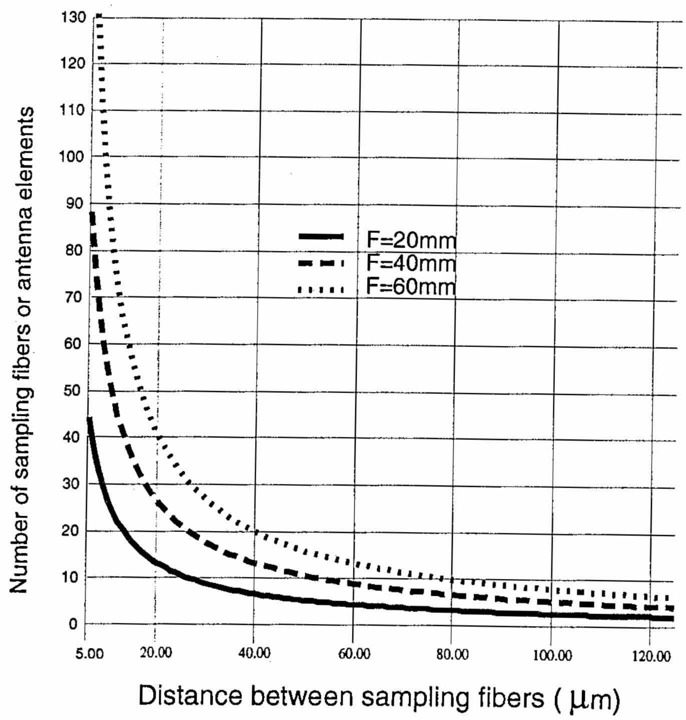

Fig. 3-6 **Variations of the number of sampling fibers or antenna elements versus the spacing between sampling fibers and the focal length of focusing lens, when λ=1.3 μm, ωo=62.5 μm**

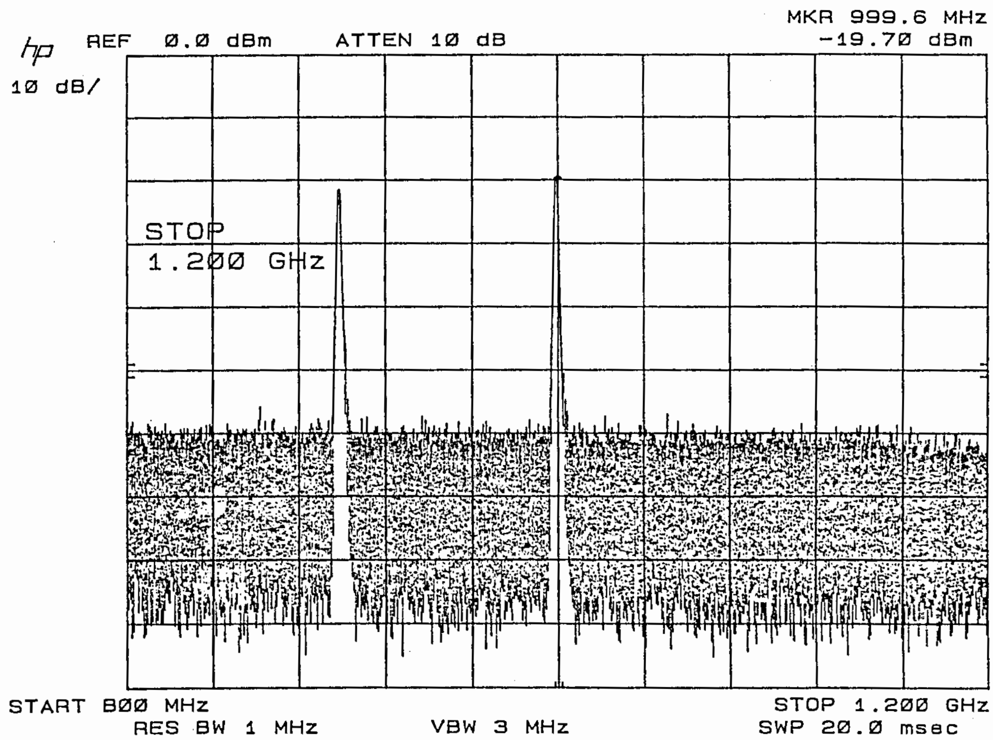

Fig. 3-7 **Detected RF signals at 900 MHz and 1 GHz from the sampling fibers located in the image plane of focusing lens.**

4. Spatial Optical Sampling Efficiency

4.1. Introduction

For the structure of the spatial optical processing array antenna as described before, the field amplitude and phase information is sampled spatially by a fiber array. This will cause optical power transmission loss, and the increase of optical-to-electric transform efficiency will be limited. In this Chapter, a method of increasing the spatial optical coupling efficiency between optical excitation beam and the optical sampling fiber bundle in the lens output image plane will be proposed by employing a periodic mesh or slit structure in the reference beam path.

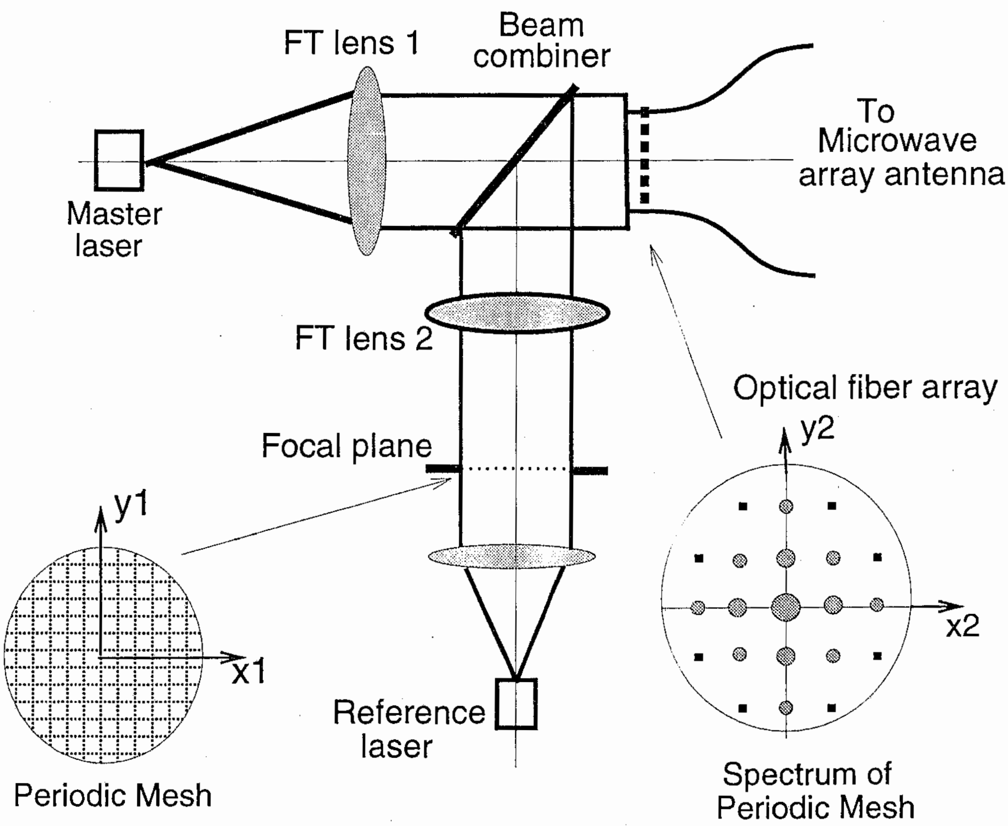

Fig. 4-1 Spatial optical processing antenna by using a periodic mesh

4.2. Diffracting Mesh

In the optical information processing, a periodic mesh is well known as a spatial modulator [24]. As shown in Fig. 4-1, by placing a mesh or a slit in one dimension in the FT lens focal plane, when a coherent source illuminates, bright spots as the Fourier spectrum image will appear in the back focal plane. If we apply a mesh in the FT lens focal plane on the reference beam path, and arrange the element of the fiber array only at the location where the bright spots appear, the spatial beam coupling efficiency is expected to be increased greatly.

For the simplicity, we consider the one dimensional problem. For a uniform transmittance on the periodic slit plane, the filed in the image plane is given as

$$E_r(x_1) = A_o \sum_{m=1}^{M} \sin c(af_x) \exp(-j2\pi mbf_x), \tag{4-1}$$

where a is the aperture size of slit, b is the distance between two slits, and $f_x = \frac{x_1}{\lambda_o F}$.

The field intensity distribution in the image plane and the relations between slit and image spots parameters are obtained as

$$I(x_1) = M^2 \sin c^2(af_x)\left(\frac{\sin(\pi Mbf_x)}{\sin(\pi bf_x)}\right)^2, \tag{4-2}$$

and

$$a = \frac{\lambda_o F}{A}, \quad b = \frac{\lambda_o F}{B}, \tag{4-3}$$

where A is the envelope size of the image filed and B is the bright spot size inside the envelope.

Fig. 4-2 illustrates the calculated field intensity distribution in the image plane and the relationship between mesh or slit and image spot parameters.

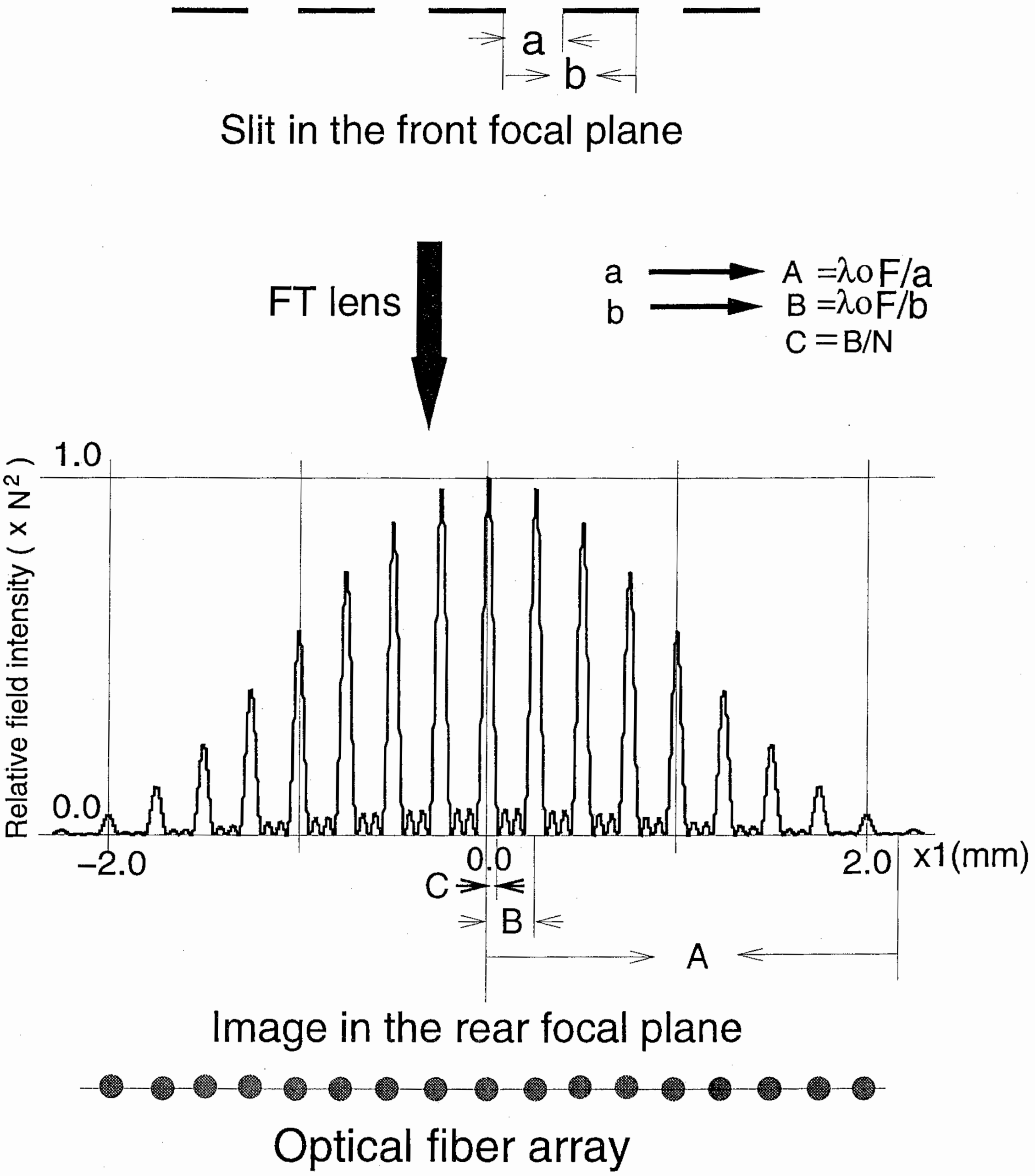

Fig. 4-2 Spectrum of the diffracting mesh

5. Summary

Based on the two-laser model of spatial Fourier optical processing techniques, a optical signal processor for multibeam microwave array antennas has been proposed in this technical report. By placing numbers of optical fibers as signal sources in the input focal plane of FT lens, and locking the laser sources to the reference laser with individual frequency offset, the multiple beams from array antenna have been produced with individual RF frequencies. This system implements the division, interconnection and combination of light spatially, this will reduce the size and complexity of BFN system greatly. Based on optical heterodyne processing and quasi-optics principles, a system design and analysis method has been given. The optical excitation field distributions and multibeam antenna radiation patterns have been calculated and simulated numerically. According to these results, the optical system parameters, such as input laser fiber position, sampling fiber array arrangement and antenna element numbers have been discussed. The beam width, field of view (FOV) and beam direction of multibeam antenna have been given in the various cases. The numerical results of system parameter simulations have shown that an extremely-wideband microwave antenna with a large beam number and array element number can be realized by using this optical processor.

The experimental system for a two-beam array antenna is designed and demonstrated. By mixing the beams from two master lasers and a reference laser with a fixed frequency offset, two RF signals at L and S bands with different phase distributions and the same Gaussian intensity distributions are detected and measured spatially. There is a very good agreement between simulated and measured results. When this optical processor is connected to a microwave array antenna, the radiation patterns and directions of the multibeam will be determined by the excitation amplitude and phase distributions, respectively. Certainly by introducing an extra signal source and a mixer, the RF signals from several GHz up to millimeter wave range could be generated.

Optoelectronic technology is making a revolutionary change worldwide in telecommunications [25], microwave and millimeter-wave engineering [26] and military radar [27]. The work shown in this technical report is a part of this dramatic research field. The design of receiving optical processing antennas, the application of Spatial Light Modulator for beam formation and the system realization for large number multibeams and elements array antennas will be our future works. As a conclusion, the relationships between optical characteristics and the requirements of phased array microwave antennas are summarized in the following.

Optical characteristics	Requirements of phased-array antennas
Working at optical frequency bands	Extreme-wide-bandwidth system
3-D signal processing and propagation capabilities	Large number beam forming
Utilization of fiber-optic technology	• Low transmission loss over long distances in the antenna feeding system • Light weight and small size
Parallelism	Simultaneous large number signal processing
Non-interference of optical signals	Immunity of electromagnetic interference and crosstalk
Fourier transform capability by optical lens	Antenna beam forming and shaping in optical domain

ACKNOWLEDGMENTS

The author gratefully acknowledge Dr. H. Inomata, Dr. Y. Karasawa and Mr. R. Miura for their encouragement and helpful discussions. I also wish to thank Mr. K. Inagaki for his very professional advice and support through this work.

REFERENCES:

[1] A. Seeds, "Opto-electronic technologies for phased array antennas: requirements, technology and application", 1994 APMC, Proc. pp.819-826.

[2] R. R. Kunath and C. A. Raquet, “NASA Lewis Research Center’s Optics-In-Antennas program”, Proc. SPIE vol.1953, Photonics for Space Environment, pp.234-242, Apr. 1993.

[3] D. K. Paul, et al., "Optical beam forming and steering technologies for satellite phased array antennas", Proc. 15th AIAA Commun. Satellite Sys. Conf., pp.1332-1341, March 1994.

[4] W. Charczenko, et al., “Integrated optical Bulter matrix for beam forming in phased array antennas”, SPIE vol.1217, Optoelectronic Signal Processing for Phased-Array Antennas II, pp.196-206, 1990.

[5] E. N. Toughlian and H. Zmuda, “Variable time delay for RF/Microwave signal processing”, SPIE vol.1476, Optical Technology for Microwave Applications V, pp.107-121, 1991.

[6] G. A. Koepf, "Optical processor for phased-array antenna beamformation", SPIE vol.477, Optical Technology for Microwave Applications, pp.75-81, May 1984.

[7] D. K. Paul, et al., "Optical beam forming and steering for phased-array antenna", Proc.1995 USNC/URSI Rasio Science Meeting, Newport Beach, CA, pp.358.

[8] 小西、中條、藤瀬、山田：“光ファイバーアレーで励振を行うアレーアンテナのビーム走査特性”、信学論（B-II）、J78-B-II, 3, pp.150-159, 1995.

[9] K. A. Nickerson, et al., “Optical processor for array antenna beam shaping and steering”, SPIE vol.1217, Optoelectronic Signal Processing for Phased-Array Antennas II, pp.184-195, 1990.

[10] L. P. Anderson, et al., "Antenna beamforming using optical processing", SPIE vol.886, Optoelectronic Signal Processing for Phased-Array Antennas, pp.228-232, 1988.

[11] 山田、千葉、唐沢："光制御アレーアンテナ給電系の周波数特性と放射実験"、信学技報, AP-95-16, pp.1-7, 1995-05.

[12] W. Birkmayer, C. Schaffer, and B. Hosselbarth, "Scenarios and system architectures advantageous for optical technologies in phased array antenna", SPIE vol. 1217, Optoelectronic Signal Processing for Phased-Array Antennas II, pp. 14-25, 1990.

[13] 小川博世, "マルチビーム衛星通信用光制御ビームフォーミングネットワークの技術動向", 信学技報, SANE95-22 (1995-06), pp.69-76.

[14] K. Horigawa, et al., "Optically controlled multiple beam forming steering network for phased array antenna", SPIE vol.2155, Optoelectronic Signal Processing for Phased-Array Antennas IV, pp.325-334, Jan. 1994.

[15] Y. Konishi, et al., "Carrier-to-noise radio and sidelobe level in a two-laser model optically controlled array antenna using Fourier optics", IEEE Trans. on Ant. and Prop., vol.40, No. 12, pp.172-178, Dec. 1992.

[16] 小西、中條、藤瀬："２台のレーザ光源をビーム形成回路に用いた光制御アレーアンテナ"、信学論（B-II）、J77-B-II, 5, pp.240-247, 1994.

[17] A. W. Rudge, et al., Editors, "The Handbook of Antenna Design", vol.1, pp.474-478, Peter Peregrinus Ltd London, 1982.

[18] Y. Ji, K. Inagaki, R. Miura and Y. Karasawa, " Spatial Fourier optical processing multi-beam array antenna", Technical Report of IEICE, AP95-80, pp.27-33, Nov. 1995.

[19] Y. Ji, K. Inagaki, R. Miura and Y. Karasawa, "Experimental Arrangement for Spatial Optical Processing Multibeam Array Antenna for Transmission", The 1996 IEICE General Conference, B-98, 28-31 March, 1996.

[20] Y. Ji, K. Inagaki, R. Miura and Y. Karasawa, "Optical feed for multibeam microwave array antennas", to be presented in 1996 IEEE AP-S International Symposium, Baltimore, USA, July 1996.

[21] H. Zmuda and E. N. Toughlian, "Adaptive microwave signal processing: A photonic solution", Microwave Journal, Vol.35, No.2, pp.58-71, Feb. 1992.

[22] M. Tamburrini, M. Parent, L. Goldberg and D. Stillwell, "Optical feed for a phased array microwave antenna", Electronics Letters, Vol.23, No.13, pp.680-681, June 1987.

[23] Y. Ji, K. Inagaki, R. Miura and Y. Karasawa, "A novel configuration of an optical processor for multibeam array antennas", to be presented in 1996 International Symposium on Antennas and Propagation (ISAP'96), Chiba, Japan, Sep. 1996.

[24] J. W. Goodman, *Introduction to Fourier Optics*, McGRAW-HILL PHYSICAL AND QUANTUM ELECTRONICS SERIES, 1968.

[25] H.Ogawa, "Technology trend in optically controlled multibeam forming network for satellite communication systems", Technical Report on IEICE, SANE95-22 (1995-06), pp.69-76.

[26] William M. Robertson, *Optoelectronic Techniques for Microwave and Millimeter-wave Engineering*, Artech House, 1995.

[27] H. Zmuda and E. N. Toughlian (Ed.), *Phtonic Aspects of Modern Radar*, Artech House, 1994.

Appendixes

Appendix 1 Gaussian Beam Optics

The fundamental mode of Gaussian beam can be written as

$$\Psi = A\frac{\omega_o}{\omega(z)}\exp(\frac{-r^2}{\omega^2(z)})\exp(-jkz)\exp(\frac{-i\pi r^2}{\lambda R(z)})\exp(i\arctan\frac{\lambda z}{\pi\omega_o^{\ 2}}). \quad \text{(A1)}$$

In Eq. (A1), the beam radius ω(z) and the curvature radius of spherical wave front R(z) are given by

$$\omega(z) = \omega_o[1+(\lambda z/\pi\omega_o^{\ 2})^2]^{0.5}, \quad \text{(A2)}$$

and

$$R(z) = z[1+(\pi\omega_o^{\ 2}/\lambda z)^2], \quad \text{(A3)}$$

respectively.

Consider a Gaussian beam transmits a lens which is usually used to focus a laser beam to a small spot, or to produce a beam of suitable diameter and phase-front curvature for injection into a given optical structure. An ideal lens leaves the transverse field distribution of a beam mode unchanged. However, a lens does change the beam parameters ω(z) and R(z). An ideal thin lens of focal length F transforms an incoming spherical wave with a radius R_1 immediately to the left of the lens into a spherical wave a radius R_2 to the right of it, where

$$\frac{1}{R_1} = \frac{1}{R_2} - \frac{1}{F}, \quad \text{(A4)}$$

Let us consider the effect of a thin lens on the propagation of a Gaussian beam with beam radius ω_o propagating to the right, as shown in Fig. A1. Because a thin lens does not affect the amplitude distribution of the field in the plane of lens, we obtain

$$\omega_{o1}[1+(\lambda d_1/\pi\omega_{o1}^{\ 2})^2]^{0.5} = \omega_{o2}[1+(\lambda d_2/\pi\omega_{o2}^{\ 2})^2]^{0.5}. \quad \text{(A5)}$$

The phase-transforming properties of the lens from Eq. (A4) yield

$$\frac{1}{d_1[1+(\pi\omega_{o1}^{\ 2}/\lambda d_1)]}+\frac{1}{d_2[1+(\pi\omega_{o2}^{\ 2}/\lambda d_2)]}=\frac{1}{F}\ . \tag{A6}$$

The two preceding equations can be solved for the output beam parameters as a function of those of the input beams, which yields

$$d_2 = F\{1+\frac{(d_1/F)-1}{[(d_1/F)-1]^2+(\pi\omega_{o1}^{\ 2}/\lambda F)^2}\}, \tag{A7}$$

and

$$\omega_{o2} = \frac{\omega_{o1}}{\sqrt{[(d_1/F)-1]^2+(\pi\omega_{o1}^{\ 2}/\lambda F)^2}}. \tag{A8}$$

From the general expressions in Eqs. (A7) and (A8), we have the following special cases:

Case 1: when d_1=F, the position of beam waist is at the focal point,
then, $d_2 = F, \quad \omega_{o2} = \frac{\lambda F}{\pi\omega_{o1}}$.

Case 2: when d_1=2F and $F \gg \omega_{o1}$, the position of beam waist is at the point of double focal length,
then, $d_2 = 2F, \quad \omega_{o2} = \omega_{o1}$.

Case 3: when $F \gg \omega_{o1}$, from Eq. (A4), we have $\frac{1}{d_2}=\frac{1}{d_1}-\frac{1}{F}$,
then, $d_1=R_1$, $d_2=R_2$.

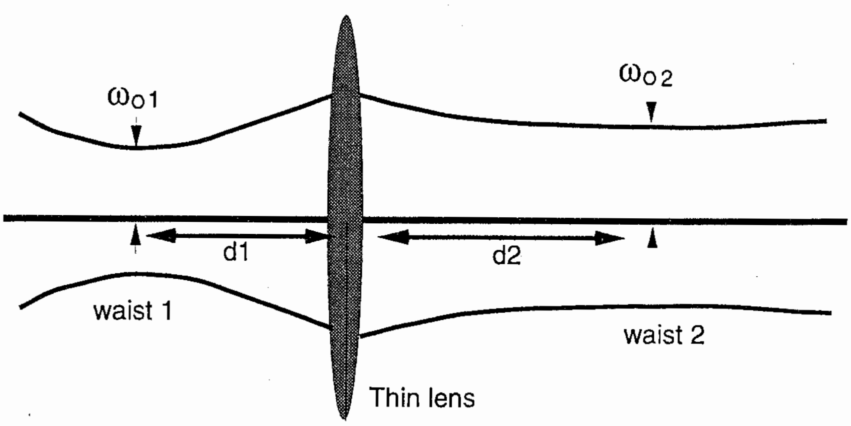

Fig. A1 The imaging of a Gaussian beam by a thin lens

Appendix 2 Laser Frequency Offset Circuit

The following laser phase-lock circuit is designed for two-beam multibeam array antennas. The same design method can be expanded to arbitrary number of beam antennas.

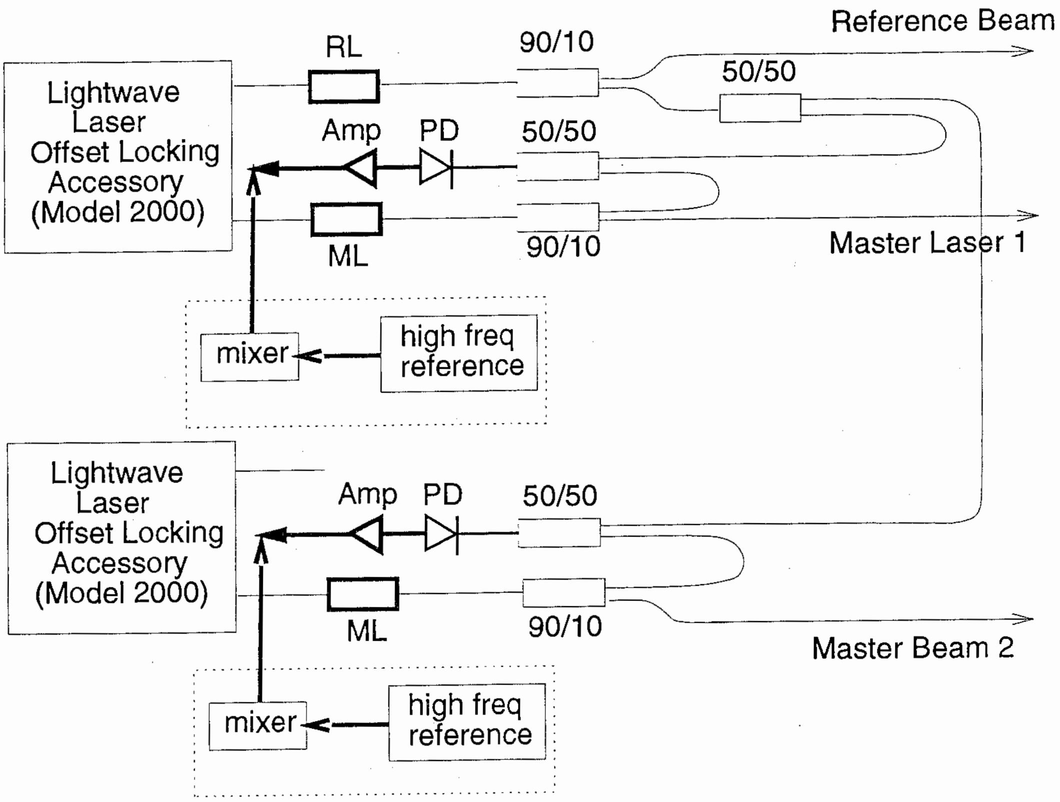

Appendix 3: Program Lists

Program 1: opdis.for

```
C        Field distribution on the image plane
C
C      -----Excitation by truncated Gaussian beams
C
C                    written by Yu Ji, ATR, 1995
C
         IMPLICIT DOUBLE PRECISION (A-H,O-Z)
         EXTERNAL FUN
         dimension ue(1000),pe(1000)
         COMMON p,ro,w0
         open(unit=12,file='p1.dat')
         open(unit=13,file='q0.dat')
C        System Parameters
C***********************************************
C        cn: number of master fibers                          *
C        x0: distance of master laser fiber from optical axis *
C        w:  diameter of fiber core                           *
C        rm: wavelength of light                              *
C        w0: beam waist                                       *
C        f:  focal length of focusing lens                    *
C        mm: number of sampling points                        *
C        ra: calculation range                                *
C        dw: interval of sampling points                      *
C***********************************************
         P=3.14159265358979323846D0
         cn=4.d0
         x0=cn*62.5d0
         w=125.d0
         A=0.d0
         B=2.d0*w/2.D0
         n=40
         rm=1.3d0
         w0=w/2.d0
         f=120000.d0
         mm=400
         ra=1000.d0
         dw=5.d0
         DO 40 J=1,mm
         t=dw*DFLOAT(J)-ra
         ro=t/(rm*f)
         CALL SIMPSON(fun,a,b,n,y)
C       Truncated Gaussian distribution
         yy=dsqrt(y**2)
         pe(j)=360.d0*x0*ro
         ue(j)=yy*cos(2.d0*p*x0*ro)
         if(umax.lt.yy) umax=yy
 40      continue
         do 30 i=1,mm
         t=dw*DFLOAT(i)-ra
C        Amplitude distribution
```

```
        z=10.*log10((ue(i)/umax)**2)
C        Phase distribution
        ph=pe(i)
        write(12,20) t,z
 20     format(2x,2f14.6)
        write(13,21) t,ph
 21     format(2x,2f14.6)
 30     continue
        close(unit=12)
        close(unit=13)
        STOP
        END
C
        DOUBLE PRECISION FUNCTION FUN(V)
        IMPLICIT DOUBLE PRECISION (A-H,O-Z)
        COMMON p,ro,w0
        X=2.d0*p*dabs(ro)*v
        CALL BESS(X,B0,B1,B2)
        gau=dexp(-v**2/w0**2)
        FUN=v*B0*gau
        RETURN
        END
C
        SUBROUTINE SIMPSON(FUN,A,B,N,SE)
        IMPLICIT DOUBLE PRECISION (A-H,O-Z)
        EXTERNAL FUN
        M=N+1
        H=(B-A)/DFLOAT(N)
        C=0.375D0
        IF(M-2) 10,10,20
     10 SE=0.5D0*(FUN(A)+FUN(B))*H
        GO TO 6
     20 IF(M-4) 40,30,40
     30 SE=0.D0
     40 IF(M/2-(M-1)/2) 1,1,2
      1 NN=M
        GO TO 3
      2 NN=M-3
      3 BB=A+DFLOAT(NN-1)*H
        SE=FUN(A)+FUN(BB)
        DO 4 I=2,NN,2
        X=A+DFLOAT(I-1)*H
      4 SE=SE+4.D0*FUN(X)+2.D0*FUN(X+H)
        SE=SE*H/3.D0
        IF(M-NN) 6,6,5
          5    SE=SE+C*H*(FUN(B-3.D0*H)+3.D0*FUN(B-2.D0*H)+3.D0*FUN(B-
H)+FUN(B))
      6 RETURN
        END
C
        SUBROUTINE BESS(X,B0,B1,B2)
        IMPLICIT DOUBLE PRECISION (A-H,O-Z)
        PARAMETER (PI=3.14159265358979323846264 3D0)
        DIMENSION AN(9),B(4),A1(9),BB1(4)
        DIMENSION A2(8),AN0(7),BN0(7)
        DIMENSION AN1(7),BN1(7)
        IF(X.EQ.0.D0)    GO TO 900
        IF(X.GT.8.D0) GO TO 1100
```

```
C
C      HART'S COEFFICIENTS FOR J0(X) 0<X<=8
       AN(1)=.28278449469808865494511 4D8
       AN(2)=-.685265989094532051592393 8D7
       AN(3)=.38831312263320038578583518D6
       AN(4)=-.9057867427723819814238153 5D4
       AN(5)=.10830696299354240019970434D3
       AN(6)=-.73483335935231405246622568D0
       AN(7)=.29212672487035592177796039D-2
       AN(8)=-.65050170570930338429093 35D-5
       AN(9)=.645380180508573442533 41D-8
       B(1)=.28278449469608718814348 5D8
       B(2)=.21695247742798797521888 3D6
       B(3)=.70046825146966788920095D3
       B(4)=1.D0
C
       AX=0.D0
       BX=0.D0
       DO 10 N=1,9
       I=N-1
       AX=AX+AN(N)*X**(2*I)
    10 CONTINUE
       DO 20 M=1,4
       K=M-1
       BX=BX+B(M)*X**(2*K)
    20 CONTINUE
       B0=AX/BX
C
C      HART'S COEFFICIENTS FOR J1(X) 0<X<=8
       A1(1)=.20401207733056935676404989D8
       A1(2)=-.24090488178461116078620946D7
       A1(3)=.89022956297134646818640971D5
       A1(4)=-.15288200237366537081586 3364D4
       A1(5)=.14404277856294376706342034D2
       A1(6)=-.80488836300867515210438521 6D-1
       A1(7)=.27202107121267732717690412D-3
       A1(8)=-.52786424969082691008128 41D-6
       A1(9)=.46597088579895764829954 3D-9
       BB1(1)=.40802415466094926655209805D8
       BB1(2)=.28220429766095254592028D6
       BB1(3)=.80886917679057948451493 1D3
       BB1(4)=1.D0
C
       AX1=0.D0
       BX1=0.D0
       DO 30 N=1,9
       I=N-1
       AX1=AX1+A1(N)*X**(2*I)
    30 CONTINUE
       AAX=X*AX1
       DO 40 M=1,4
       K=M-1
       BX1=BX1+BB1(M)*X**(2*K)
    40 CONTINUE
       B1=AAX/BX1
C
       IF(X.GT.4.D0) GO TO 1000
C
```

```
C       TAYLOR EXPANSION FOR BESSLE J2(X) 0=<X<=4
        A2(1)=9.99999999976749D-1
        A2(2)=-3.333333325890460D-1
        A2(3)=4.166666275260593D-2
        A2(4)=-2.777769924370040D-3
        A2(5)=1.157329859141126D-4
        A2(6)=-3.302705428488350D-6
        A2(7)=6.764094810589540D-8
        A2(8)=-8.945896939133650D-10
        X2=X/2.D0
        AR=0.D0
        DO 50 N=1,8
        I=N-1
        AR=AR+A2(N)*X2**(2*I)
   50 CONTINUE
        B2=AR*X2*X2/2.D0
        RETURN
C       FOR X>4.
C
 1000 B2=2.D0*B1/X-B0
        RETURN
 1100 CONTINUE
C       FOR X>=8.
C
        X8=8.D0/X
        X4=X-PI/4.D0
        R=DSQRT(2.D0/PI/X)
        X41=X-3.D0*PI/4.D0
C
C      HART'S COEFFICIENTS FOR J0(X) X>=8
        AN0(1)=.9999999999999565129D0
        AN0(2)=-.1098632766989088D-2
        AN0(3)=.27380101973018D-4
        AN0(4)=-.21738794671755D-5
        AN0(5)=.345410268934D-6
        AN0(6)=-.722808953D-7
        AN0(7)=.10674427321D-7
        BN0(1)=-.1562499999695619D-1
        BN0(2)=.143051115362161D-3
        BN0(3)=-.6930230212988D-5
        BN0(4)=.820160220725D-6
        BN0(5)=-.169498248529D-6
        BN0(6)=.41517915237D-7
        BN0(7)=-.6636866261D-8
        PO=0.D0
        QQ=0.D0
        DO 11 N=1,7
        I=N-1
        PO=PO+AN0(N)*X8**(2*I)
   11 CONTINUE
        DO 21 M=1,7
        K=M-1
        QQ=QQ+BN0(M)*X8**(2*K)
   21 CONTINUE
        QX=QQ*X8
        B0=R*(PO*DCOS(X4)-QX*DSIN(X4))
C
C       HART'S COEFFICIENTS FOR J1(X) X>=8
```

```
      AN1(1)=1.0000000000004746D0
      AN1(2)=.183105463785442D-2
      AN1(3)=-.3520314112486D-4
      AN1(4)=.257541348131D-5
      AN1(5)=-.39221954096D-6
      AN1(6)=.8048531455D-7
      AN1(7)=-.1178079374D-7
      BN1(1)=.4687499999966953D-1
      BN1(2)=-.20027157161617D-3
      BN1(3)=.84703580079D-5
      BN1(4)=-.9465978801D-6
      BN1(5)=.18986975764D-6
      BN1(6)=-.4581656636D-7
      BN1(7)=.727402264D-8
      P1=0.D0
      Q1=0.D0
      DO 15 N=1,7
      I=N-1
      P1=P1+AN1(N)*X8**(2*I)
   15 CONTINUE
      DO 25 M=1,7
      K=M-1
      Q1=Q1+BN1(M)*X8**(2*K)
   25 CONTINUE
      QX1=Q1*X8
      B1=R*(P1*DCOS(X41)-QX1*DSIN(X41))
      B2=2.D0*B1/X-B0
      RETURN
C
C      FOR X=0.000D0
  900 B0=1.D0
      B1=0.D0
      B2=0.D0
      RETURN
      END
```

Program 2. nopdis.for

```
C       Optical field distribution on the image plane
C     -----Excitation by Gaussian beams
C
        dimension ue(2500),pe(2500)
        open(unit=12,file='p0.dat')
        open(unit=13,file='q0.dat')
C       System Parameters
C*****************************************************
C       cn: number of master fibers                  *
C       x0: distance of master laser fiber from optical axis *
C       w:   diameter of fiber core                  *
C       rm: wavelength of light                      *
C       w0: beam waist                               *
C       f:   focal length of focusing lens           *
C       mm: number of sampling points                *
C       ra: calculation range                        *
C       dw: interval of sampling points              *
C*****************************************************
        P=3.14159265358979323846
        cn=2.0
        x0=cn*62.5
        w=125.0
        rm=1.3
        w0=w/2.
        f=40000.
        mm=2000
        ra=1000.
        dw=1.d0
        DO 40 J=1,mm
        t=dw*FLOAT(J)-ra
        ro=t/(rm*f)
C     Gaussian distribution
        yy=exp(-(p*w0*ro)**2)
        pe(j)=360.*x0*ro
        ue(j)=yy*cos(2.*p*x0*ro)
        if(umax.lt.yy) umax=yy
 40     continue
        do 30 i=1,mm
        t=dw*FLOAT(i)-ra
C       Amplitude distribution
        z=10.*log10((ue(i)/umax)**2)
C       Phase distribution
        ph=pe(i)
        write(12,20) t,z
 20     format(2x,2f14.6)
        write(13,21) t,ph
 21     format(2x,2f14.6)
 30     continue
        close(unit=12)
        close(unit=13)
        STOP
        END
```

Program 3: pa.for

```
C        Radiation pattens of an optical processing multibeam array antenna
C
C     -----Excitation by truncated Gaussian beams
C
C                    written by Yu Ji, ATR, 1995
C
         IMPLICIT DOUBLE PRECISION (A-H,O-Z)
         EXTERNAL FUN
         dimension ue(2000),ph(2000)
         dimension pat1(2000),pat2(2000),pattern(2000),the(2000)
         COMMON p,ro,w0
         open(unit=12,file='pr1.dat')
         P=3.14159265358979323846
C Parameters in the optical processing part
C*******************************************************
C        x0: distance of master laser fiber from optical axis        *
C        w:    diameter of fiber core                                *
C        rm: wavelength of light                                     *
C        w0: beam waist                                              *
C        f:    focal length of focusing lens                         *
C        mm: number of sampling fibers                               *
C*******************************************************
         x0=0.d0
         w=125.d0
         A=0.d0
         B=w/2.D0
         n=40
         rm=1.3d0
         w0=w/2.d0
         f=40000.d0
         dw=125.0d0
         mm=9
         ra=dfloat((mm-1)/2)*dw
C    Parameters in the microwave array antenna part
C********************************************************
C        dm=wavelength/2                                              *
C********************************************************
         DO 40 J=1,mm
         t=dw*DFLOAT(J-1)-ra
         ro=t/(rm*f)
         CALL SIMPSON(fun,a,b,n,y)
         ph(j)=2.d0*p*x0*ro
         ue(j)=dabs(y)
 40      continue
         do 10 k=2,1800
         theta=p*dfloat(k-1)/1800.d0-p/2.d0
         the(k)=theta*180.d0/p
         do 30 i=1,mm
         ai=dfloat(i-(mm-1)/2)
         angle=p*ai*dsin(theta)
         pat1(k)=pat1(k)+ue(i)*dcos(theta)*cos(angle-ph(i))
         pat2(k)=pat2(k)+ue(i)*dcos(theta)*sin(angle-ph(i))
 30      continue
         pattern(k)=dsqrt(pat1(k)**2+pat2(k)**2)
```

```
       pp=pattern(k)
       if(pmax.lt.pp) pmax=pp
 10    continue
       write(*,*) pmax
       pm=pmax
       do 50 kk=2,1800
       th=the(kk)
       patt=20.d0*dlog10(pattern(kk)/pm)
       write(12,20) th,patt
 20    format(2x,2f14.6)
 50    continue
       close(unit=12)
       STOP
       END
CC
       DOUBLE PRECISION FUNCTION FUN(V)
       IMPLICIT DOUBLE PRECISION (A-H,O-Z)
       COMMON p,ro,w0
       X=2.d0*p*dabs(ro)*v
       CALL BESS(X,B0,B1,B2)
       gau=dexp(-v**2/w0**2)
       FUN=v*B0*gau
       RETURN
       END
C
       SUBROUTINE SIMPSON(FUN,A,B,N,SE)
C*******************************************
C Integral caculation by SIMPSON method            *
C*******************************************
       IMPLICIT DOUBLE PRECISION (A-H,O-Z)
       EXTERNAL FUN
       M=N+1
       H=(B-A)/DFLOAT(N)
       C=0.375D0
       IF(M-2) 10,10,20
   10 SE=0.5D0*(FUN(A)+FUN(B))*H
       GO TO 6
   20 IF(M-4) 40,30,40
   30 SE=0.D0
   40 IF(M/2-(M-1)/2) 1,1,2
    1 NN=M
       GO TO 3
    2 NN=M-3
    3 BB=A+DFLOAT(NN-1)*H
       SE=FUN(A)+FUN(BB)
       DO 4 I=2,NN,2
       X=A+DFLOAT(I-1)*H
    4 SE=SE+4.D0*FUN(X)+2.D0*FUN(X+H)
       SE=SE*H/3.D0
       IF(M-NN) 6,6,5
         5    SE=SE+C*H*(FUN(B-3.D0*H)+3.D0*FUN(B-2.D0*H)+3.D0*FUN(B-
H)+FUN(B))
    6 RETURN
       END
C
```

```
      SUBROUTINE BESS(X,B0,B1,B2)
C************************************************
C   Caculation of BESSEL function (J0,J1,J2)       *
C************************************************
      IMPLICIT DOUBLE PRECISION (A-H,O-Z)
      PARAMETER (PI=3.14159265358979323846264 3D0)
      DIMENSION AN(9),B(4),A1(9),BB1(4)
      DIMENSION A2(8),AN0(7),BN0(7)
      DIMENSION AN1(7),BN1(7)
      IF(X.EQ.0.D0)   GO TO 900
      IF(X.GT.8.D0) GO TO 1100
C
C      HART'S COEFFICIENTS FOR J0(X) 0<X<=8
      AN(1)=.28278449469808865494 5114D8
      AN(2)=-.68526598909453205159 23938D7
      AN(3)=.38831312263320038578583518D6
      AN(4)=-.90578674277238198142381535D4
      AN(5)=.10830696299354240019970434D3
      AN(6)=-.73483335935231405246622568D0
      AN(7)=.29212672487035592177796039D-2
      AN(8)=-.65050170570930338429 09335D-5
      AN(9)=.64538018050857344253341D-8
      B(1)=.28278449469608718814 3485D8
      B(2)=.21695247742798797521 8883D6
      B(3)=.70046825146966788920095D3
      B(4)=1.D0
C
      AX=0.D0
      BX=0.D0
      DO 10 N=1,9
      I=N-1
      AX=AX+AN(N)*X**(2*I)
   10 CONTINUE
      DO 20 M=1,4
      K=M-1
      BX=BX+B(M)*X**(2*K)
   20 CONTINUE
      B0=AX/BX
C
C      HART'S COEFFICIENTS FOR J1(X) 0<X<=8
      A1(1)=.20401207733056935676404989D8
      A1(2)=-.24090488178461116078620946D7
      A1(3)=.89022956297134646818640971D5
      A1(4)=-.15288200237366537081586 3364D4
      A1(5)=.14404277856294376706342034D2
      A1(6)=-.80488836300867515210 4385216D-1
      A1(7)=.27202107121267732717690412D-3
      A1(8)=-.52786424969082691008 12841D-6
      A1(9)=.46597088579895764829 9543D-9
      BB1(1)=.40802415466094926655209805D8
      BB1(2)=.28220429766095254592028D6
      BB1(3)=.80886917679057948451493 1D3
      BB1(4)=1.D0
      AX1=0.D0
      BX1=0.D0
      DO 30 N=1,9
      I=N-1
      AX1=AX1+A1(N)*X**(2*I)
```

```
   30 CONTINUE
      AAX=X*AX1
      DO 40 M=1,4
      K=M-1
      BX1=BX1+BB1(M)*X**(2*K)
   40 CONTINUE
      B1=AAX/BX1
      IF(X.GT.4.D0)  GO TO 1000
C
C      TAYLOR EXPANSION FOR BESSLE J2(X) 0=<X<=4
      A2(1)=9.99999999976749D-1
      A2(2)=-3.333333325890460D-1
      A2(3)=4.166666275260593D-2
      A2(4)=-2.777769924370040D-3
      A2(5)=1.157329859141126D-4
      A2(6)=-3.302705428488350D-6
      A2(7)=6.764094810589540D-8
      A2(8)=-8.945896939133650D-10
      X2=X/2.D0
      AR=0.D0
      DO 50 N=1,8
      I=N-1
      AR=AR+A2(N)*X2**(2*I)
   50 CONTINUE
      B2=AR*X2*X2/2.D0
      RETURN
C      FOR X>4.
C
 1000 B2=2.D0*B1/X-B0
      RETURN
 1100 CONTINUE
C      FOR X>=8.
C
      X8=8.D0/X
      X4=X-PI/4.D0
      R=DSQRT(2.D0/PI/X)
      X41=X-3.D0*PI/4.D0
C     HART'S COEFFICIENTS FOR J0(X) X>=8
      AN0(1)=.9999999999999565129D0
      AN0(2)=-.1098632766989088D-2
      AN0(3)=.2738010197301 8D-4
      AN0(4)=-.21738794671755D-5
      AN0(5)=.345410268934D-6
      AN0(6)=-.722808953D-7
      AN0(7)=.10674427321D-7
      BN0(1)=-.1562499999695619D-1
      BN0(2)=.143051115362161D-3
      BN0(3)=-.6930230212988D-5
      BN0(4)=.820160220725D-6
      BN0(5)=-.169498248529D-6
      BN0(6)=.41517915237D-7
      BN0(7)=-.6636866261D-8
      PO=0.D0
      QQ=0.D0
      DO 11 N=1,7
      I=N-1
      PO=PO+AN0(N)*X8**(2*I)
   11 CONTINUE
```

```
      DO 21 M=1,7
      K=M-1
      QQ=QQ+BN0(M)*X8**(2*K)
   21 CONTINUE
      QX=QQ*X8
      B0=R*(PO*DCOS(X4)-QX*DSIN(X4))
C      HART'S COEFFICIENTS FOR J1(X) X>=8
      AN1(1)=1.0000000000004746D0
      AN1(2)=.183105463785442D-2
      AN1(3)=-.3520314112486D-4
      AN1(4)=.257541348131D-5
      AN1(5)=-.39221954096D-6
      AN1(6)=.8048531455D-7
      AN1(7)=-.1178079374D-7
      BN1(1)=.4687499999966953D-1
      BN1(2)=-.20027157161617D-3
      BN1(3)=.84703580079D-5
      BN1(4)=-.9465978801D-6
      BN1(5)=.18986975764D-6
      BN1(6)=-.4581656636D-7
      BN1(7)=.727402264D-8
      P1=0.D0
      Q1=0.D0
      DO 15 N=1,7
      I=N-1
      P1=P1+AN1(N)*X8**(2*I)
   15 CONTINUE
      DO 25 M=1,7
      K=M-1
      Q1=Q1+BN1(M)*X8**(2*K)
   25 CONTINUE
      QX1=Q1*X8
      B1=R*(P1*DCOS(X41)-QX1*DSIN(X41))
      B2=2.D0*B1/X-B0
      RETURN
C      FOR X=0.000D0
  900 B0=1.D0
      B1=0.D0
      B2=0.D0
      RETURN
      END
```

Program 4: npa.for

```
C       Radiation pattens of an optical processing multibeam array antenna
C
C     -----Excitation by Gaussian beams
C
C                   written by Yu Ji, ATR, 1995
C
        dimension ue(2000),ph(2000)
        dimension pat1(2000),pat2(2000),pattern(2000),the(2000)
        open(unit=12,file='pr0.dat')
        P=3.14159265358979323846D0
C   Parameters in the optical processing part
C*******************************************************
C       x0: distance of master laser fiber from optical axis      *
C       w:   diameter of fiber core                               *
C       rm: wavelength of light                                   *
C       w0: beam waist                                            *
C       f:   focal length of focusing lens                        *
C       mm: number of sampling fibers                             *
C*******************************************************
        x0=0.0
        w=12.0
        rm=1.3
        w0=w/2.0
        f=120000.0
        dw=125.0
        mm=9
        ra=float((mm-1)/2)*dw
C   Parameters in the microwave array antenna part
C*******************************************************
C       dm=wavelength/2                                           *
C*******************************************************
        DO 40 J=1,mm
        t=dw*FLOAT(J-1)-ra
        ro=t/(rm*f)
        ph(j)=2.0*p*x0*ro
        ue(j)=exp(-(p*w0*ro)**2)
 40     continue
        do 10 k=2,1800
        theta=p*float(k-1)/1800.0-p/2.0
        the(k)=theta*180.0/p
        do 30 i=1,mm
        ai=float(i-(mm-1)/2)
        angle=p*ai*sin(theta)
        pat1(k)=pat1(k)+ue(i)*cos(theta)*cos(angle-ph(i))
        pat2(k)=pat2(k)+ue(i)*cos(theta)*sin(angle-ph(i))
 30     continue
        pattern(k)=sqrt(pat1(k)**2+pat2(k)**2)
        pp=pattern(k)
        if(pmax.lt.pp) pmax=pp
 10     continue
        write(*,*) pmax
        pm=pmax
        do 50 kk=2,1800
        th=the(kk)
```

```
      patt=20.0*log10(pattern(kk)/pm)
      write(12,20) th,patt
20    format(2x,2f14.6)
50    continue
      close(unit=12)
      STOP
      END
```